

1 Date: April 17, 2020

2

3 Subject: Cover Letter for Revised Submission of bg-2019-508

4

5 Dear Reviewers and Associate Editor,

6

7 We thank you all for taking time to provide thoughtful and constructive comments. We have
8 addressed all comments, and paid particular attention to (1) clarify new concepts such as
9 relative sif, (2) expand our concluding recommendations with more detailed strategies to
10 improve model formulation and model-observational analysis, and (3) benchmarking analysis
11 against stand along tower driven SCOPE simulations. The resulting manuscript is improved in
12 readability and outcomes.

13

14 Please find below our merged document containing comments from Reviewers 1 and 2 with
15 embedded Author Responses and Changes (Page 2-10) and Tracked Changes starting on Page
16 11. Note the line numbers in the Reviewer comments (black font) refer to our original
17 submission, while Page and line numbers in the Author Response (blue font) refer to the
18 "Tracked Changes" document below.

19

20 Best regards,

21

22

23

24

25

26 Dr Nicholas Parazoo (on behalf of all co-authors)

27 Jet Propulsion Laboratory

28 4800 Oak Grove Drive

29 Mail Stop 200-233

30 Pasadena, CA 91109

31 Phone: 818.354.2973

32

1 Comments and Author Response to Reviewer 1:

2

3 General: Parazoo et al. compare seven SIF-enabled TBMs against empirical SIF and GPP data
4 from a subalpine evergreen coniferous forest. The models, which had SIF retro-fitted, share
5 some common concepts but on the other hand differ widely in terms of other concepts, with
6 corresponding impacts on simulated SIF. The authors describe the differences compared to the
7 empirical data and discuss these in terms of the differences in model structure.

8

9 Interest in the adding SIF capabilities to TBMs is largely driven by the recent availability of
10 global SIF satellite products which provides promising avenues for additional constraints on
11 carbon cycling, especially for GPP. Given that this research field is still in its infancy, I think the
12 scope of this study, even though limited to a single site and a few weeks of peak-vegetation
13 period data, is justified. The manuscript is well written and I think the authors do a great job in
14 navigating the reader through the complexity of the investigated TBMs without getting lost in
15 the many aspects these models differ.

16

17 [We thank the reviewer for the nice feedback and helpful comments, and for appreciating our](#)
18 [decision to keep our scope of study limited. Our hope is to build off the baseline findings](#)
19 [reported here.](#)

20

21 I have only really very few detailed comments (see below) and only one major comment, that is
22 that I was wondering whether the model comparison would profit from adding simulations with
23 the original SCOPE model. This model is some sort of golden standard for SIF modelling (in fact
24 many of the investigated models have gleaned from SCOPE in one way or the other) and I could
25 imagine that SCOPE simulations might provide a good benchmark for the investigated TBMs,
26 which given their scope need to weigh complexity against realism. Even though SCOPE is much
27 more complex in terms of the treatment of canopy radiative transfer and gas exchange, running
28 it with pre-scribed meteo inputs and adjusting a few key parameters should be easy to do.

29

30 [This was a great recommendation and worth the extra effort. We now include results from](#)
31 [SCOPE v1.73 with prescribed met input for the year of study \(2017\) and vegetation parameters](#)
32 [\(LA, canopy height, leaf chlorophyll content, and Vcmax\) calibrated to NR1 according to Raczka](#)
33 [et al., 2019. Results from the stand-alone version of SCOPE are quite similarly qualitatively and](#)
34 [quantitatively to the coupled version with BETHY \(high bias in APAR and SIF\), except with](#)
35 [improved diurnal and synoptic variability compared to PhotoSpec. This provides a nice](#)
36 [benchmark for TBM-SIFs in this study. We provide a description of SCOPE in the methods,](#)
37 [references to SCOPE results throughout, and plots of SCOPE in all relevant figures \(including](#)
38 [Figs 2-5 in the main text\).](#)

39

40 Detailed comments:

41 I. 60: and theoretical models suggest a non-linear response at leaf-scale (Gu et al. 2019)

42

43 [Statement added as follows:](#)

1 “Spaceborne data indicate a linear relationship between SIF and GPP at large spatial (kilometer)
2 and temporal (bi-weekly) scales (e.g., Sun et al., 2017) for several ecosystems, while theoretical
3 models and ground-based measurements indicate a more non-linear relationship at leaf and
4 canopy scales (Zhang et al., 2016; Gu et al., 2019; van der Tol et al., 2014; Magney et al., 2017,
5 2019a).

6
7 I. 84: a needle is anatomically a leaf

8
9 Changed ‘needle/leaf’ to ‘leaf’

10
11 I. 102: not so much at leaf-scale really

12
13 Changed ‘leaf to canopy scale’ to ‘canopy scale’

14
15 I. 103: the FLOX is missing in the list of tower-mounted spectrometer systems

16
17 added FLOX and reference to Shan et al., 2019 and Julitta et al., 2017

18 Shan, N., Ju, W., Migliavacca, M., Martini, D., Guanter, L., Chen, J., Goulas, Y., Zhang, Y.:
19 Modeling canopy conductance and transpiration from solar-induced chlorophyll
20 fluorescence. *Agricultural and Forest Meteorology*, 268, 189–201, 2019.

21 Julitta, T., Burkart, A., Colombo, R., Rossini, M., Schickling, A., Migliavacca, M., Cogliati, S.,
22 Wutzler, T., Rascher, U.: Accurate measurements of fluorescence in the O2A and O2B band
23 using the FloX spectroscopy system - results and prospects. In: *Proc. Potsdam GHG Flux
24 Workshop: From Photosystems to Ecosystems, 24–26 October 2017, Potsdam, Germany.*
25 <https://www.potsdam-flux-workshop.eu/>, 2017

26 Fig. 1: calling a 3-year average a climatology is a bit of a stretch in my view – maybe
27 just refer to this as the 2015-2018 average?

28
29 Yes, thank you

30
31 I. 165-174: how representative are these measurements for the larger footprint of the
32 flux tower?

33
34 Under most daytime conditions and turbulent boundary layers, SIF measurements have a much
35 smaller footprint compared to eddy covariance data, and thus are typically not representative
36 of the larger ecosystem. We added the following stipulation at the end of the paragraph:

37
38 “We note that APAR measurements are only as representative as the distribution of PAR
39 sensors beneath the canopy; while they are placed within the footprint of SIF (Sec 2.2.3) and
40 fetch of eddy covariance (Sec 2.2.4) measurements, they cannot be a perfect representation of
41 canopy APAR for each eddy covariance and SIF measurement.”

1
2 I. 229: one sentence on the effects of complex terrain, for which NR1 is famous, on
3 NEE and inferred GPP?
4
5 Good point. The location does not have a significant impact on daytime fluxes, but we added
6 the following sentence for full disclosure.
7
8 “We note the tower location near the Continental Divide in the Rocky Mountains of Colorado
9 does present slope flow challenges for eddy covariance during nighttime, but the relatively flat
10 area of the tower reduces impact on daytime flux measurements (Burns et al., 2018).”
11
12 Burns, S. P., Swenson, S. C., Wieder, W. R., Lawrence, D. M., Bonan, G. B., Knowles, J. F., and
13 Blanken, P. D.: A comparison of the diel cycle of modeled and measured latent heat flux
14 during the warm season in a Colorado subalpine forest, *Journal of Advances in Modeling
15 Earth Systems*, 10, 617–651, 2018.

16
17 I. 260: wouldn't that be the Ball-Berry-Woodrow (BBW) model?
18 I. 261: and this simply the Leuning model?
19
20 Corrected in Sec 2.3.2 and in Table 1
21
22 Table 1: what is the difference between big-leaf and single layer models? Where do
23 two-leaf big-leaf models fall into?
24
25 Thank you for pointing out these differences. The models can be classified as follows.
26
27 BETHY = multiple layers (sunlit/shaded)
28 ORCHIDEE/SIB3/4 = big leaf (sunlit only)
29 CLM4.5/5 = two big leaf (sunlit/shaded)
30 BEPS = two leaf (sunlit/shaded)
31
32 We clarify these differences in Table 1 and in Section 2.3.1 as shown below
33
34 “These differences, which are summarized in Table 1, include the representation of stomatal-
35 conductance (all use Ball-Berry except CLM5.0, BEPS, and ORCHIDEE), canopy absorption of
36 incoming radiation (all account for sunlit/shaded radiation except ORCHIDEE, SIB3, and SIB4),
37 limiting factors for photosynthesis (V_{cmax} , LAI, radiation, stress) and SIF (k_N , fluorescence
38 photon re-absorption), scaling and radiative transfer methods for transferring leaf-level SIF
39 simulations to top of canopy, and parameter optimization.”
40
41 I. 573: sunlit/shaded leaf area fractions
42
43 corrected, thank you

1
2
3
4
5
6
7
8
9
10
11
12
13
14
15
16
17
18
19
20
21
22
23
24
25
26
27
28
29
30
31
32
33
34
35
36
37
38
39
40
41
42

I. 803-810: what are recommendations for model structure with respect to APAR?

We added the following recommendation at the end of Area 1 of Section 5, keeping in mind the stipulation that there is really no perfect in situ APAR measurement:

“We recommend further site-level investigation of observed and simulated canopy light absorption, emphasizing comparison of multi-layer and multi-leaf radiation schemes accounting for sunlit and shaded leaf area.”

I. 816: might refer to new approaches such as stomatal optimisation based on xylem hydraulics (Eller et al. 2020)

Agreed. We added the following recommendation at the end of Area 2 of Section 5:

“We also recommend more inclusion of stomatal optimization models (e.g., Eller et al., 2020) as optional parameterizations for TBMs, to better account for plant hydraulic functioning under water stress compared to the more widely used semi-empirical models.”

I. 821: here I would think we also need more data from a wider variety of plant species under in situ conditions, especially all kinds of stress, ideally combining active and passive chlorophyll fluorescence measurements

Agreed. We added the following recommendation at the end of Area 3 of Section 5:

“We also emphasize a need for more simultaneous measurements of active and passive chlorophyll fluorescence to determine the temporal dynamics of competing pathways (PQ, NPQ) from a wider variety of plant species under ambient conditions and different levels of stress.”

I. 833: for perspective - do the authors dare to say something about what they would expect from a similar model comparison for a well-watered high-LAI crop?

We added a 6th bullet point at the end of Section 5:

“Finally, we note that our focus on a water limited subalpine evergreen needleleaf forest represents a challenging case study for models and observations. In many cases, there is strong covariance between LAI, SIF, APAR and GPP in cropping systems (Dechant et al., 2020), but because this study site experiences little change in canopy structure and APAR throughout the season (Magney et al, 2019b), our study sought to provide more explicit insight into the models sensitivity to photosynthesis and fluorescence. As such, it is possible that we would see more convergence of results, and a reduction in confounding effects (e.g., decreased NPQ), in a well-

1 watered high-LAI cropping system. We therefore recommend similar model-observation
2 assessments across a wider range of biota and climate.”

3
4

1 Comments and Author Response to Reviewer 1:

2

3 This paper compares different process based terrestrial biosphere model (TBMs) that include
4 solar induced chlorophyll fluorescence (SIF) as output. The models are briefly introduced, with
5 emphasis on the different representations of SIF. The model output with respect to SIF and
6 gross primary productivity (GPP) output is inter-compared, and comparisons are made to a time
7 series of field measurements. The models diverged, and the authors relate the differences
8 among the models to the underlying process descriptions: the estimates of APAR, energy
9 partitioning in the leaf and radiative transfer of fluorescence.

10

11 The paper provides a good overview of current TBMs capable of simulating SIF. This is of
12 interest to the readers. It has an informative title, abstract and figures. It does not introduce
13 new concepts, but it compares existing model concepts and recommends strategies for
14 improvement. The paper is well written and clear. I have the following recommendations to
15 consider in the preparation of the final manuscript (all minor):

16

17 [Thank you for the very kind review.](#)

18

19 1. Make the paper (even) more inviting for readers who are unfamiliar with the terminology of
20 SIF. In Line 208, SIF_{yield} is first used, later in lines 593-602, it is defined, and the difference
21 with SIF_{rel} is discussed. It may be helpful to introduce SIF_{yield}, SIF_{rel} and phi_F together
22 and earlier, explaining why these three are used for comparison in this paper (in Figs 3 and
23 4), and what they mean.

24

25 [We thank the reviewer for this helpful suggestion. We added a new section \(2.2.2\) toward the
26 beginning of the methods to clarify these differences, merging information from line 208 and
27 593-602.](#)

28

28 ["2.2.2 SIF Yield](#)

29

30 We define and clarify three important quantities that define the relationship between absorbed
31 light and emitted SIF at leaf and canopy scales. ϕ_F is the quantum yield of fluorescence,
32 representing the probability an absorbed photon will be fluoresced. This quantity can be
33 observed at leaf level using PAM fluorimetry, or calculated by models as a function of rate
34 coefficients for energy transfer (Sec 2.3.3). SIF_{yield} is the canopy emitted SIF per photon absorbed.
35 The quantify is estimated from models and observations as the ratio of absolute canopy SIF and
36 APAR (SIF_{canopy}/APAR). SIF_{yield} is our best attempt to account for the effect of (a) canopy absorbed
37 light and (b) SIF re-absorption within the canopy on the canopy integrated emission of SIF.
38 However, factors such as observation angle, fraction of sunlit/shaded canopy components, and
39 difference in footprint from APAR, necessitates an additional diagnostic variable defined as
40 relative SIF (SIF_{rel}). SIF_{rel} is emitted SIF per reflected radiance in the far red spectrum where SIF
41 retrievals occur (SIF/Ref_{fr}). This is useful because is normalizes for the exact amount of
42 'illuminated' canopy elements within the sensor field of view, whereas APAR measurements are
42 integrated for the entire canopy.

1 These quantities represent different but equally important versions of reality. It is difficult for
2 models to exactly reproduce the distribution and timing of sunlight in the canopy as observed by
3 PhotoSpec. While SIF_{rel} removes model-observations differences in illumination, it confounds our
4 interpretation of the relationship with GPP_{yield} , which is derived from APAR. As such, we provide
5 both results to be comprehensive, but note the temporal stability associated with SIF_{rel} as the
6 more physical interpretation of canopy yield for this short period of study.”

7

8 2. Lines 623-626. I did not grasp the following reasoning: ‘Finally, we note that PhotoSpec
9 scans of leaf-level emissions are averaged and reported here as canopy averages, while
10 model output is reported at the top of the canopy, which accounts for within-canopy
11 radiative transfer, re-absorption of SIF, and shaded canopies, causing lower emissions
12 compared to the canopy average.’ Aren’t the top-of-canopy measurements also affected by
13 within-canopy radiative transfer etcetera?
14

15 Thank you for pointing out this source of confusion. We clarify as follows (Page 34, Line 4-19):

16

17 “Finally, we clarify an important difference between observed and predicted estimates of canopy
18 average SIF. PhotoSpec scans direct emissions from sunlit and shaded leaves within the canopy,
19 thus observing the ‘total’ emission from leaves in the instrument FOV. We then average each of
20 these leaf-level scans and report as canopy averages. Model output, in contrast, is reported at
21 the TOC, which represents the ‘net’ emission from leaves after attenuation in the canopy
22 (through canopy radiative transfer, re-absorption of SIF, and shading). Assuming sunlit and
23 shaded leaves within the canopy emit at the same rate as TOC leaves, attenuation will reduce the
24 effective signal from leaf-level emissions within the canopy. As such, the average of leaf level
25 emissions (canopy average) is expected to be lower than the net emission of leaves reaching the
26 top of canopy.

27 This is important because CLM4.5 shows strong attenuation of SIF from leaf-level to TOC,
28 decreasing by a factor of 2-3 at midday (Fig S7). The interpretation here is that the model bias in
29 absolute SIF may actually be higher than reported here; however, we note that more quantitative
30 information on the observed fraction of sunlit vs shaded leaves and comparative top-of-canopy
31 SIF values for the same canopy elements are needed (to account for off-nadir SIF viewing) for
32 more accurate determination of scaling between observed canopy and top-of-canopy SIF.”

33 3. Continuation of previous point: The difference between the measurements and the
34 simulations is that the measurements are the average of small footprints at multiple viewing
35 angles, whereas the models are nadir values, as explained in the ‘apples to apples’ section (line
36 691). I presume the radiative transfer factor τ_{740} was derived from SCOPE simulations in nadir.
37 With SCOPE it is possible to estimate $\tau_{740}(\theta)$ for multiple observation angles, and then take
38 the average. Thus it is possible to compare apples to apples. I understand the TBM’s do not
39 have this right now, but at least I would have expected that to be part of the discussion, or as
40 part of recommendation 5, which now only mentions instruments with a wider FOV.

41

42 Very excellent point. We added the following sentence to area 5 of Section 5

43

1 “More effort is also needed to better align models with observations, for example by leveraging
2 three-dimensional capabilities in SCOPE (and other RTMs) to directly account for multiple
3 observation angles.”

4
5 4. Line 566, Strictly, x is not the fraction of absorbed light not used in photosynthesis, if this
6 refers to the variable ‘ x ’ in the model of Lee et al. and Van der Tol, because when $x = 0$, this
7 fraction is 0.17 due to constitutive heat dissipation.

8
9 Thank you for clarifying. We removed the statement that x refers to the “fraction of absorbed
10 light not used in photosynthesis”

11
12 5. Line 728-730. ‘The fact that relative SIF is the least sensitive [] reduces the sensitivity to APAR
13 and reveals a strong SIF response to changes in photochemical quenching’. Yes, that seems to
14 be the case, but perhaps a few lines can be added to guide the reader through this argument
15 (see also point 1).

16
17 We agree this is a difficult concept to grapple with. We try to clarify as follows (Page 38, Line 4-
18 10):

19
20 “Our results indicate a wide range of SIF responses to APAR: TBM-SIFs and SCOPE are usually far
21 too sensitive to APAR, observations of absolute SIF are less sensitive, and observations of
22 relative SIF (SIF_{rel}) are least sensitive (Fig. 5D). We remind the reader that SIF_{rel} is normalized by
23 the amount of far red light reflected from leaves in the FOV of PhotoSpec, and thus has reduced
24 sensitivity to absorbed light than absolute SIF. The fact that SIF_{rel} is the least sensitive to APAR
25 means other processes are driving changes in SIF under increased light absorption. In this case,
26 it reveals a strong SIF response to changes in photochemical quenching.”

27
28 6. Line 811, recommendation 2. Is it the water stress formulation, or the parameter values, i.e.
29 the values for the Ball-Berry parameters?

30
31 Here, we are referring to different kinds of the stomatal conductance models (ball-berry,
32 leuning) and water stress (e.g., soil moisture scalar for attenuating conductance). We clarify
33 (Page 41, Line 7-9)

34
35 “The underlying photosynthetic models fail to simulate the magnitude of depression of
36 observed GPP in the afternoon, regardless of how stomatal-conductance and water stress
37 models and parameters are formulated”

38
39 Following Reviewer 1, we also advocate for more use of stomatal optimization models (Page 41,
40 Line 13-16)

41
42 “We also recommend more inclusion of stomatal optimization models (e.g., Eller et al., 2020) as
43 optional parameterizations for TBMs, to better account for plant hydraulic functioning under
44 water stress compared to the more widely used semi-empirical models.”

1
2
3 7. In Line 680, there is a reference to Figure 6, which is not in the manuscript
4
5 [Good catch, we refer to Fig S8 now.](#)
6
7 8. Figure 3C and 3D. What is the temporal resolution of these data? Multiple-day averages? It
8 takes some effort to relate the spikes to the wet and dry periods described in the text.
9
10 [Thank you. We have clarified the temporal resolution in the text and figure caption.](#)
11
12 Technical comments
13
14 Line 290, sentence starting 'The quantum yield' has an extra 'to':
15 Line 365 and elsewhere, I recommend to spell out 'met forcing':
16 Line 508, 'eaves' should be 'leaves':
17 Figures S1 and S4 are reversed:
18 The labels in Figure S7 are too small
19 The legend in Figure S8 is too small
20
21 [All corrected](#)
22

1 Wide Discrepancies in the Magnitude and Direction of Modelled SIF in Response to Light
2 Conditions

3
4 Nicholas C Parazoo¹, Troy Magney^{1,2}, Alex Norton³, Brett Raczka⁴, Cédric Bacour⁵, Fabienne
5 Maignan⁶, Ian Baker⁷, Yongguang Zhang⁸, Bo Qiu⁸, Mingjie Shi⁹, Natasha MacBean¹⁰, Dave R.
6 Bowling⁴, Sean P. Burns^{11,12}, Peter D. Blanken¹¹, Jochen Stutz⁹, Katja Grossman¹³, Christian
7 Frankenberg^{1,2}

8
9 Jet Propulsion Laboratory, California Institute of Technology¹

10 California Institute of Technology²

11 School of Earth Sciences, University of Melbourne³

12 School of Biological Sciences, University of Utah⁴

13 NOVELTIS, 153 rue du Lac, 31670 Labège, France⁵

14 Laboratoire des Sciences du Climat et de l'Environnement, LSCE/IPSL⁶

15 Colorado State University⁷

16 International Institute for Earth System Sciences, Nanjing University, China⁸

17 University of California Los Angeles⁹

18 Department of Geography, Indiana University¹⁰

19 Department of Geography, University of Colorado¹¹

20 National Center for Atmospheric Research¹²

21 Institute of Environmental Physics, University of Heidelberg¹³

22
23 Prepared for Biogeosciences
24

1 **Abstract:**

2 Recent successes in passive remote sensing of far-red solar induced chlorophyll fluorescence (SIF)
3 have spurred development and integration of canopy-level fluorescence models in global
4 terrestrial biosphere models (TBMs) for climate and carbon cycle research. The interaction of
5 fluorescence with photochemistry at the leaf- and canopy- scale provides opportunities to
6 diagnose and constrain model simulations of photosynthesis and related processes, through
7 direct comparison to and assimilation of tower, airborne, and satellite data. TBMs describe key
8 processes related to absorption of sunlight, leaf-level fluorescence emission, scattering and
9 reabsorption throughout the canopy. Here, we analyze simulations from an ensemble of process-
10 based TBM-SIF models (SiB3, SiB4, CLM4.5, CLM5.0, BETHY, ORCHIDEE, BEPS) and the SCOPE
11 canopy radiation and vegetation model at a subalpine evergreen needleleaf forest near Niwot
12 Ridge, Colorado. These models are forced with local meteorology and analyzed against tower-
13 based continuous far-red SIF and gross primary productivity (GPP) partitioned eddy covariance
14 data at diurnal and synoptic scales during the growing season (July-August 2017). Our primary
15 objective is to summarize the site-level state of the art in TBM-SIF modeling over a relatively short
16 time period (summer) when light, canopy structure, and pigments are similar, setting the stage
17 for regional- to global-scale analyses. We find that these models are generally well constrained
18 in simulating photosynthetic yield, but show strongly divergent patterns in the simulation of
19 absorbed photosynthetic active radiation (PAR), absolute GPP and fluorescence, quantum yields,
20 and light response at leaf and canopy scale. This study highlights the need for mechanistic
21 modeling of non-photochemical quenching in stressed and unstressed environments, and
22 improved representation of light absorption (APAR), distribution of sunlit and shaded light, and
23 radiative transfer from leaf to canopy scale.

Deleted: relating

Deleted: tower observed

Deleted: ical data,

24

25

1 Section 1: Introduction

2 Our ability to estimate and measure photosynthesis beyond the leaf scale is extremely limited.
3 This inhibits the ability to evaluate the performance of terrestrial biosphere models (TBMs) that
4 are designed to quantify the direct impact and feedbacks of the carbon cycle with climate change.
5 Consequently, there are substantial uncertainties in estimating the gross primary production
6 (GPP) response to environmental changes and carbon-climate feedback (Friedlingstein et al.,
7 2014). Global, multi-scale remote sensing of solar induced fluorescence (SIF) may represent a
8 major breakthrough in alleviating this deficiency (Mohammed et al, 2019). Spaceborne data
9 indicate a linear relationship between SIF and GPP at large spatial (kilometer) and temporal (bi-
10 weekly) scales (e.g., Sun et al., 2017) for several ecosystems, while [theoretical models and](#)
11 ground-based measurements indicate a more non-linear relationship at leaf and canopy scales
12 (Zhang et al., 2016; Gu et al., 2019; van der Tol et al., 2014; Magney et al., 2017, 2019a).

13 Chlorophyll fluorescence is re-emitted energy produced during the photosynthetic light
14 reactions, in which a small fraction (roughly 2%) of photosynthetic active radiation (PAR)
15 absorbed by chlorophyll is re-emitted at longer wavelengths (650-850 nm) as fluorescence. In
16 ambient conditions, the emission of SIF represents a by-product of two primary de-excitation
17 pathways, photochemical and nonphotochemical quenching (PQ, NPQ). Plants have evolved
18 these regulatory mechanisms to prevent damage to photosynthetic machinery when the amount
19 of absorbed radiation is greater than that which can be used to drive photochemistry. Chlorophyll
20 fluorescence responds dynamically to changes in photochemistry and NPQ from instantaneous
21 to hourly, daily, and seasonal timescales, as a function of changing environmental conditions and
22 plant structural properties (Porcar-Castell et al., 2014; Demmig-Adams et al., 2012). SIF is
23 fundamentally different than steady-state fluorescence yield typically measured at the leaf scale
24 as it is sensitive to both changes in photochemistry as well as absorbed PAR (APAR, related to
25 incident light, canopy structure, and biochemical content). The response of canopy SIF to APAR
26 is well documented in deciduous and evergreen forests and cropping ecosystems (Yang et al.,
27 2018; Badgley et al, 2017; Miao et al., 2018; Magney et al., 2019b; Li et al., 2020). More recently,
28 Magney et al. (2019b) showed that seasonal changes in canopy SIF for cold climate evergreen

1 systems is influenced by changes in needle physiology and photoprotective pigments (Magney et
2 al., 2019b).

3 To properly account for these factors, process-based SIF models must represent these underlying
4 non-linear biophysical and chemical processes. Several modeling groups have adapted TBMs to
5 incorporate various SIF formalisms for the purpose of model evaluation, data assimilation, and
6 improved model prediction (Lee et al., 2015; Koffi et al., 2015; Thum et al., 2017; Norton et al.,
7 2019; Bacour et al., 2019; Raczka et al., 2019). With these goals in mind, TBM SIF modeling
8 requires two important steps: (1) a representation of SIF at the leaf scale that accounts for NPQ
9 and photochemistry, and (2) canopy radiative transfer of SIF, which enables a comparison to large
10 field-of-view observations (e.g. tower, satellites). The second step involves accounting for
11 radiative transfer within the canopy and has typically relied on incorporating the Soil Canopy
12 Observation Photosynthesis Energy model (SCOPE, van der Tol et al., 2009, 2014), which
13 simulates chlorophyll fluorescence as a function of biophysics, canopy structure, environmental
14 conditions, and sun/sensor geometries. This approach has been adopted by TBMs in various ways
15 using different assumptions for fluorescence modeling and radiative transfer, as will be discussed
16 in Section 2.

17 Typically, measuring chlorophyll fluorescence and competing pathways (PQ, NPQ) has been done
18 at the leaf scale via pulse-amplitude modulation fluorescence (PAM, Schreiber et al., 1986).
19 Recently, commercially available spectrometers have made it possible to measure SIF directly in
20 the field at the leaf and canopy scale, and also enable the study of structural, environmental, and
21 directional controls (Cogliati et al. 2015; Daumard et al. 2010; Migliavacca et al. 2017; Yang et al.
22 2015; Grossman et al., 2018; [Aasen et al., 2019](#); Gu et al., 2019b; Zhang et al., 2019). The use of
23 field deployable instruments on eddy covariance towers has increased rapidly since 2014,
24 providing coverage of multiple vegetation types across various climates around the world (Yang
25 et al., 2018; Magney et al., 2019a,b; Parazoo et al., 2019). These data enable improved
26 understanding of the relationship between SIF, GPP, APAR, and environmental effects at canopy
27 scales. Novel tower-mounted spectrometer systems such as Fluospec2 (Yang et al., 2018),
28 [Photospec](#) (Grossman et al., 2018), [and FLOX](#) (e.g., [Julitta et al., 2017](#); [Shan et al., 2019](#)) have
29 made it possible to monitor canopy SIF continuously in the field with high precision over multiple

Deleted: needle/

Deleted: leaf to

Deleted: and

Deleted:

1 years providing opportunities for more direct comparison and evaluation of satellite data
2 (Grossman [et al.](#), 2018; Yang [et al.](#), 2015, 2018; [Wohlfahrt et al., 2018](#); Magney et al., 2019).
3 PhotoSpec offers the additional benefits (and challenge) of (a) precise field of view capable of
4 resolving leaf-level SIF, and (b) canopy scanning at azimuth and elevation angles. These features
5 enable SIF integration from leaf- to canopy- scales, and interpretation of directional variations of
6 the emitted radiance.

7 Canopy scanning spectrometers such as PhotoSpec thus provide an opportunity to understand
8 the physical processes that lead to a breakdown of SIF-GPP linearity at leaf to canopy scale (or
9 conversely, emergence of linearity at increasing scale), and for detailed evaluation and diagnosis
10 of TBM performance. This study provides a preliminary benchmarking site-level assessment for
11 simulations of SIF within a TBM framework and across an ensemble of TBMs, with the primary
12 purpose being an initial investigation into the response of modelled SIF and GPP to light during
13 peak summer. We leverage continuous measurements of SIF and GPP at the Niwot Ridge US-NR1
14 Ameriflux flux tower in Colorado from June-July 2017 (Magney et al., 2019b), [and simulations of](#)
15 [canopy radiative transfer, photosynthesis, and fluorescence from a stand-alone version of SCOPE,](#)
16 to (1) Benchmark TBM-SIF modeling, (2) Evaluate sensitivity to underlying processes and scaling
17 techniques, (3) Identify strengths and weaknesses in current modeling strategies, and (4)
18 Recommend strategies for models and observations.

19 The paper is organized as follows: Section 2 describes [SCOPE and](#) the seven TBM-SIF models (SiB3,
20 SiB4, ORCHIDEE, BEPS, BETHY, CLM4.5, CLM5) which have recently been published or are in
21 review, and provides more details on site level benchmarking observations. Section 3 summarizes
22 results comparing modelled and predicted SIF and GPP at hourly and daily scales, as they relate
23 to absorbed light, GPP and SIF yields, and quantum yields. Section 4 discusses results in more
24 detail, including attribution of SIF magnitude and temporal phasing biases and sensitivities to
25 absorbed light, and areas for improvement.

26 **Section 2: Methods**

27 *2.1 Site: Niwot Ridge, Colorado*

1 Our study focuses on an AmeriFlux (<https://ameriflux.lbl.gov/>) site in Niwot Ridge, Colorado,
2 USA (US-NR1), where a tower-based eddy covariance system has been continuously measuring
3 the net ecosystem exchange of carbon dioxide (NEE) over a high-elevation subalpine forest
4 since 1999, and a spectrometer system that has been continuously monitoring SIF since June
5 2017 (Grossman et al., 2018; Magney et al., 2019b). The 26 m tall tower is located in a high
6 elevation forest (3050 m asl) located in the Rocky Mountains of Colorado (Burns et al., 2015; Hu
7 et al., 2010; Monson et al., 2002) and consists primarily of the evergreen species of lodgepole
8 pine (*Pinus contorta*), Engelmann spruce (*Picea engelmannii*), and subalpine fir (*Abies*
9 *lasiocarpa*). The mean annual temperature is 1.5°C and mean annual precipitation is 800 mm
10 (65% as snow). The forest is roughly 120 years old with a mean canopy height of 11.5 m, and a
11 leaf area index of 4.2 m² m⁻². More site-specific details can be found in Burns et al. (2015).

12 At Niwot Ridge, interannual variations in GPP are closely linked to winter snowfall amount, which
13 typically melts by early June, and summer precipitation, characterized by afternoon convective
14 thunderstorms triggered by upslope flow (Burns et al., 2015; Albert et al., 2017) and
15 climatological peak precipitation around 2 pm local time (Fig 1A). We note that our study period
16 of July-August 2017 is unusual for NR1 (relative to the 2015-2018 mean) in its bimodal
17 distribution of diurnal precipitation (morning and afternoon peaks), lower than normal afternoon
18 precipitation, cooler temperatures, and reduced vapor pressure deficit (Fig 1 A-C). The early
19 morning peak is due to a strong storm system that moved through from July 22-24 (Fig 1E), and
20 does not show up when these days are removed. This period also shows a decrease in incoming
21 shortwave relative to climatology despite lower precipitation (Fig 1D). We note that a second
22 storm passed through in early August. The combination of these two storms produced net
23 decreases in air temperature (Fig 1F), vapor pressure deficit (Fig 1G) and sunlight (Fig 1H) over a
24 two-week period from late July to early August.

25 2.2 Tower-Based Measurements: PAR, SIF, CO₂ Flux

26 2.2.1 Absorbed PAR

27 The site is equipped with two main upward-facing PAR sensors. The first (LICOR LI-190R),
28 mounted on the PhotoSpec telescope unit, provides an independent measurement of

Deleted: -

1 direct/diffuse light and can be used to calibrate PhotoSpec (Grossman et al., 2018). The second
2 (SQ-500-SS; Apogee Instruments), mounted on the main flux tower, is part of a larger array of
3 upward- and downward-oriented PAR sensors above and below the canopy used for the
4 calculation of the fraction of PAR absorbed by the vegetation canopy (fAPAR). The two PAR
5 sensors show a similar diurnal pattern during July-August 2017 (Fig S1), including an afternoon
6 dip and relatively smaller values overall compared to 2018 (the only other year with available
7 PAR for comparison).

8 Full-spectrum quantum sensors (SQ-500-SS; Apogee Instruments) were new and factory-
9 calibrated together just before installation. Above-canopy sensors (one up and one down-facing)
10 were mounted on the main flux tower, and below-canopy sensors (six up and six down) were
11 mounted at the 2 m height above ground on a shorter canopy-access towers. APAR was
12 calculated for each pair of below-canopy relative to above-canopy sensors for every half-hour,
13 then averaged among sensors over daylight hours to create a daytime average. We then estimate
14 hourly APAR by multiplying hourly incoming PAR (measured and integrated from 400-700 nm) at
15 the top of canopy (PAR) by the daytime average of fAPAR. Fig S2 shows the mean diurnal cycle
16 for July-August 2017 for each sensor, and the across-sensor average, with APAR data collection
17 beginning on July 13, 2017. We note that APAR measurements are only as representative as the
18 distribution of PAR sensors beneath the canopy; while they are placed within the footprint of SIF
19 (Sec 2.2.3) and fetch of eddy covariance (Sec 2.2.4) measurements, they cannot be a perfect
20 representation of canopy APAR for each eddy covariance and SIF measurement.

21 2.2.2 Fluorescence parameters

22 We define and clarify three important quantities that define the relationship between absorbed
23 light and emitted SIF at leaf and canopy scales. ϕ_F is the quantum yield of fluorescence,
24 representing the probability an absorbed photon will be fluoresced. This quantity can be
25 observed at leaf level using PAM fluorimetry or calculated by models as a function of rate
26 coefficients for energy transfer (Sec 2.3.3). SIF_{yield} is the canopy emitted SIF per photon absorbed.
27 The quantity is estimated from models and observations as the ratio of absolute canopy SIF and
28 APAR ($SIF_{canopy}/APAR$). SIF_{yield} is our best attempt to account for the effects of (a) canopy absorbed
29 light and (b) SIF re-absorption within the canopy on the canopy integrated emission of SIF.

1 However, factors such as observation angle, fraction of sunlit/shaded canopy components, and
2 difference in footprint from APAR, necessitates an additional diagnostic variable defined as
3 relative SIF (SIF_{rel}). SIF_{rel} is emitted SIF per reflected radiance in the far red spectrum where SIF
4 retrievals occur (SIF/Ref_r). This is useful because is normalizes for the exact amount of
5 'illuminated' canopy components within the sensor field of view, whereas APAR measurements
6 are integrated for the entire canopy.

7 These quantities represent different but equally important versions of reality. It is difficult for
8 models to exactly reproduce the distribution and timing of sunlight in the canopy as observed by
9 PhotoSpec. While SIF_{rel} removes model-observation differences in illumination, it confounds our
10 interpretation of the relationship with GPP_{yield} , which is derived from APAR. As such, we provide
11 both results to be comprehensive, but note the temporal stability associated with SIF_{rel} as the
12 more physical interpretation of canopy yield for this short period of study.

13 2.2.3 Tower Based Measurements of Solar Induced Chlorophyll Fluorescence (SIF)

14 SIF data has been collected from a scanning spectrometer (PhotoSpec) installed at the AmeriFlux
15 US-NR1 tall tower since June 17, 2017. PhotoSpec sits atop the tower at 26 m above the ground
16 and roughly 15 m above the forest canopy top, transferring reflected sunlight and SIF data
17 collected from the needleleaf canopy through a tri-furcated optical cable to three spectrometers
18 in a shed at the base of the tower. These spectrometers measure far-red fluorescence in the 745-
19 758 nm retrieval window at high spectral resolution (FWHM = 0.3 nm) and with a 0.7 deg field of
20 view (FOV), resulting in a 20 cm diameter footprint at nadir on top of the canopy. The far-red SIF
21 data are then scaled to 740 nm for model intercomparison using the first principal component of
22 the spectral shape in Magney et al., 2019a. Photospec scans from nadir to the horizon in 0.7
23 degrees steps at two azimuth directions, with a time resolution of ~20 s per measurement and
24 complete scan time of 20 minutes. For this study, we aggregate scans across all azimuth and
25 elevation angles into hourly, canopy level averages to benchmark model estimates of top of
26 canopy (TOC) or canopy averaged SIF (BETHY only, see Sec 2.3.4.1) at diurnal and synoptic time
27 scales. We refer the reader to Grossman et al. (2018) and Magney et al (2019b) for further details
28 regarding PhotoSpec, implementation at US-NR1, and data filtering. We focus our model-data

Deleted: 2

Deleted: -

Deleted: A two-month data collection gap in fall of 2017 limits our ...

1 analysis on the 2017 growing season (July-August, 2017) to maximize overlap between
2 observations of SIF, GPP, and APAR.

Deleted: to

3 Diurnal composites of PhotoSpec SIF in 2017 show a late morning peak and afternoon dip (Fig
4 S3A). The afternoon dip is consistent with decreased incoming shortwave, PAR and APAR (Figs S1
5 and S2, respectively). However, we note the retrieved signal from PhotoSpec is also affected by
6 (1) viewing geometry, (2) fraction of sunlit vs shaded leaves (sun/shade fraction, i.e. the quantity
7 of needles illuminated by incident sunlight) due to self-shading within the canopy, and (3)
8 direct/diffuse fraction due to cloud cover. Structural and bidirectional effects lead to different
9 SIF emission patterns depending on view angle and scanning patterns (Yang and van der Tol,
10 2018). The viewing geometry of PhotoSpec (as implemented at NR1 in 2017) causes a higher
11 fraction of illuminated vegetation in the morning, which leads to a 2 to 3 hour offset in the timing
12 of peak SIF (Fig S3A) and incoming far-red reflected radiance within the retrieval window (Fig
13 S3B), from the peak zenith angle of the sun at noon (coinciding with the expected peak in PAR)
14 to late morning. Normalizing SIF by far-red reflected radiance as relative SIF (SIF_{rel} , Fig S3C) and
15 rescaling to SIF (Fig S3D) shifts the peak back to noon and preserved the afternoon dip (albeit
16 with reduced magnitude). SIF_{rel} helps to account for factors 1-3 listed above because it accounts
17 for the amount of reflected radiation in the field of view of PhotoSpec, which is impacted by
18 canopy structure, sun angle, and direct/diffuse light. As discussed above, SIF_{rel} is likely a better
19 approximation of SIF_{yield} because it normalizes for the exact amount of 'illuminated' canopy
20 components in each retrieval, whereas APAR integrates the entire canopy. As such, we expect
21 SIF_{rel} to have a strong seasonal change associated with downregulation of photosynthesis, and a
22 more subtle diurnal change, as during mid-summer the SIF signal is primarily driven by light
23 intensity.

Deleted: we are

Deleted: ing

Deleted: elements

Deleted: the

Deleted: measurements are

Deleted: d for

24 It is important to note that the PhotoSpec system is highly sensitive to sun/shade fraction in the
25 canopy (factor 2) due to the narrow FOV of the PhotoSpec telescoping lens. Increased afternoon
26 cloud cover during summer causes diurnal asymmetry in incident PAR (Fig S1A). We examine this
27 effect in more detail (Section 3) by analyzing SIF and GPP under clear and diffuse sky conditions
28 using a threshold (0.5, top-of-canopy/top-of-atmosphere incoming shortwave radiation) similar
29 to that used in Yang et al. (2017) and Yang et al. (2018).

2.2.4 CO₂ Flux and GPP Partitioning

NEE measurements are screened using u_{star} filtering, and partitioned into gross primary production (GPP) and terrestrial ecosystem respiration components using the so-called nighttime method which is based on the relationship between NEE during the nighttime ($\text{PAR} < 50 \text{ } \mu\text{mol m}^{-2} \text{ s}^{-1}$) and air temperature (Reichstein et al., 2005). Diurnal averages of GPP based on nighttime partitioning show similar diurnal structure to PAR and SIF including the afternoon dip and reduced overall magnitude compared to the 2015-2018 mean (Fig S4). Similar results are found using daytime light partitioning of NEE (Lasslop et al., 2010; Fig S4) and thus only nighttime partitioned GPP data are reported for the remainder of this study. All GPP estimates are processed as half hourly means, then gap filled and averaged hourly. We note the tower location near the Continental Divide in the Rocky Mountains of Colorado presents slope flow challenges for eddy covariance during nighttime, but the relatively flat area of the tower reduces impact on daytime flux measurements (Burns et al., 2018). Details on the flux measurements, data processing and quality control are provided in Burns et al. (2015).

Deleted: 3

2.3 Modeling Approach

2.3.1 TBM-SIF Overview

The parent TBMs are designed to simulate the exchanges of carbon, water, and energy between biosphere and atmosphere, from global to local scales depending on inputs from meteorological forcing, soil texture, and plant functional type. The addition of a fluorescence model that simulates SIF enables a direct comparison to remotely sensed observations for benchmarking, process diagnostics, and parameter/state optimization (data fusion) for improved GPP estimation. The TBM-SIF models analyzed here differ in ways too numerous to discuss. We refer the reader to the appropriate references in Section 2.3.4 for more detailed model descriptions. Instead, we focus on key differences affecting joint simulation of GPP and leaf/canopy level SIF at diurnal and synoptic scale, during the peak of summer. These differences, which are summarized in Table 1, include the representation of stomatal-conductance (all use Ball-Berry except CLM5.0, BEPS, and ORCHIDEE), canopy absorption of incoming radiation (all account for sunlit/shaded radiation except ORCHIDEE, SiB3, and SiB4), limiting factors for photosynthesis

Commented [NCP1]: Dave/Sean – This is in response to R1 (Wolffahrt) regarding EC uncertainty in mountains. I stole this wording from the 2018 paper, please reword as needed.

1 (V_{cmax} , LAI, radiation, stress) and SIF (k_N , [fluorescence photon re-absorption](#)), scaling and radiative
2 transfer methods for transferring leaf-level SIF simulations to top of canopy, and parameter
3 optimization. Further details on (a) photosynthetic structural formulation and parameter choice,
4 (b) representation of leaf level processes important to SIF (k_N and ϕ_P), and (c) leaf-to-canopy
5 scaling approach (SIF_{canopy}) are provided in Sections 2.3.2 and 2.3.3.

6 2.3.2 Photosynthesis Models

7 All TBM-SIF models in this manuscript used enzyme-kinetic models to simulate leaf assimilation
8 rate (gross photosynthesis) as limited by the efficiency of photosynthetic enzyme system, the
9 amount of PAR captured by leaf chlorophyll, and the capacity of leaves to utilize end products of
10 photosynthesis (Farquhar et al., 1980; Collatz et al., 1991, 1992; Sellers et al., 1996). However,
11 there are important differences in the representation of (a) stomatal conductance that couples
12 carbon/water cycles, and (b) limiting factors on carbon assimilation due to leaf physiology
13 (maximum carboxylation capacity, V_{cmax}), radiation (APAR or fAPAR), canopy structure (LAI, leaf
14 angle distribution), and stress (water supply and demand, temperature), that affect plant
15 physiological processes and canopy radiative transfer. The underlying stomatal conductance
16 models in the TBMs analyzed here are represented by the Ball-Berry family of empirical models
17 rooted in the leaf gas exchange equation but with different representations of atmospheric
18 demand (relative humidity or vapor pressure deficit), including the Ball-Berry-[Woodrow](#) model
19 (Ball et al., 1987), the [Leuning model](#) (Leuning, 1995), the Yin-Stuik model (Yin and Struik, 2009),
20 and the Medlyn model (Medlyn et al., 2011). These structural and parametric differences also
21 influence calculated values such as the degree of light saturation (Section 2.3.3), which influence
22 both the fluorescence and quantum yield as used by the fluorescence models. Differences in
23 stomatal conductance, canopy type / radiation scheme, stress, V_{cmax} , and LAI are summarized in
24 Table 1.

25 2.3.3 Fluorescence Modeling Approach

26 Following the general approach described in Lee et al. (2015) and van der Tol et al. (2014), the
27 flux of total leaf-level emitted fluorescence, SIF_{leaf} , can be diagnosed using a light use efficiency
28 framework analogous to the expression for photosynthesis (Monteith et al., 1972),

Formatted: Subscript

Formatted: Subscript

Deleted: Ball-Berry-

Formatted: Subscript

$$\begin{aligned}
 SIF_{leaf} &= fAPAR * PAR * \phi_F \\
 &= APAR * \phi_F
 \end{aligned}
 \tag{Equation 1}$$

where PAR and $fAPAR$ are defined in Section 2.2.1 but measured at leaf level, and ϕ_F is the quantum yield of fluorescence, representing the number of photons emitted by fluorescence per absorbed photon. We note that photosystems I and II (PSI and PSII, respectively) contribute to leaf level fluorescence but only PSII is considered in models analyzed here (with the exception of ORCHIDEE and BETHY, Section 2.3.4.2). ϕ_F is estimated as follows:

$$\phi_F = \frac{k_F}{k_F + k_D + k_N} (1 - \phi_p)
 \tag{Equation 2}$$

where k represents the rate coefficients for the different pathways for the transfer of energy from excited chlorophyll (k_F = fluorescence, k_D = heat dissipation, and k_N = non-photochemical quenching, or NPQ), and ϕ_p is the quantum yield of electron transport (see Section 2.3.2). k_F is typically set to a constant value (0.05) in models following van der Tol et al (2014). k_D is also typically set to a constant value of 0.95, or temperature corrected in some cases (e.g., ORCHIDEE, CLM4.5, CLM5.0, BETHY). k_N has a substantial and variable impact on energy partitioning at diurnal and seasonal scales which varies as a function of light saturation (e.g., Raczka et al., 2019; Porcar-Castell et al., 2011). Once leaf level emissions are known, an approach is needed estimate the total TOC fluorescence flux (SIF_{canopy}) for comparison to Photospec data. Leaf and canopy level fluorescence modeling is described in more detail in Section 2.3.3.1 and 2.3.3.2 below.

2.3.3.1 Leaf level SIF emission

The ‘quantum yield’ approach has been used in SIF models to characterize the fraction of photons that are used for PQ, NPQ, or re-emitted as fluorescence (van der Tol 2014). It is important to note, that this does not translate into the actual amount of SIF emission leaving the leaf, but is used as an approximation. TBM-SIF models typically represent ϕ_p using lake model formalism, which assumes large connectivity between photosynthetic units (Genty et al., 1989; van der Tol et al., 2014). ϕ_p is expressed in terms of the degree of light saturation (x), derived from the native photosynthesis module of the parent TBM and represents the balance between actual and potential electron transport rates, and the maximum photochemical yield under dark-acclimated

Deleted: to

1 conditions (ϕ_{pmax}), which is derived from the fluorescence model and defined in terms of rate
2 coefficients in Eq 2.

3 ϕ_N accounts for the ability of plants to dissipate excess energy as heat via NPQ through the
4 regulation of xanthophyll cycle pigments (Demmig-Adams and Adams, 2006). NPQ can be
5 represented as a sum of reversible (k_R) and sustain (k_S) components ($k_N = k_R + k_S$). k_R accounts for
6 the relatively fast (diurnal), reversible NPQ response to light. k_S accounts for the relatively slow
7 (seasonal), sustained NPQ response to light and other environmental factors. With the exception
8 of CLM4.5, models do not typically account for k_S .

9 A significant challenge in fluorescence models is to find an appropriate relationship between k_N
10 and the degree of light saturation (x). The TBM-SIF models represent k_N through an approach
11 similar to the one used in SCOPE, which uses a parametric model of k_N derived from PAM
12 fluorometry measurements (van der Tol et al., 2014).

13 NPQ models can be classified as stressed (drought) and unstressed relative to water availability
14 depending on the dataset from which empirical fits are derived. The unstressed model is ideal
15 for irrigated systems such as crops, and the stressed model is more appropriate for water limited
16 ecosystems such as Niwot Ridge. We examine each of these models using drought and unstressed
17 models from van der Tol (2014), and a drought-based model from Flexas et al. (2002). These
18 models use different empirical fits but are otherwise identical. In general, k_N increases more
19 rapidly with APAR (light saturation), and ramps up to a higher level, in the drought-based model
20 compared to the unstressed model. Additionally, some models provide unique improvements
21 such as dependence on environmental conditions (e.g., water stress vs no water stress in
22 ORCHIDEE), and equations for reversible and sustained NPQ to represent the different time
23 scales (minutes to seasonal) at which NPQ regulation occurs (e.g., CLM4.5) influenced by
24 pigmentation changes in the leaf.

25 2.3.3.2 Leaf-to-Canopy scaling

26 The TBM-SIFs produce leaf-level fluorescence which needs to be converted to canopy-level
27 fluorescence (SIF_{canopy}) to be directly compared to PhotoSpec and satellite observations. Leaf- to
28 canopy- level conversion of SIF requires a representation of canopy radiative transfer, which in

1 general is too computationally expensive to include within the TBMs in this study, that are
2 designed for global scale application. Therefore, most TBMs analyzed here account for canopy
3 radiative transfer of SIF using some representation of SCOPE (van der Tol 2009a,b). The most
4 commonly used approach is to run independent simulations of SIF from SCOPE to create an
5 empirical conversion factor (κ_{740}) between leaf and canopy level SIF that is a function of V_{cmax}
6 (Lee et al., 2015). This conversion factor accounts for integration over the fluorescence emission
7 spectrum, observation angle, and unit conversion. Model variations of this empirical approach,
8 as well as additional approaches utilizing the full SCOPE model and a SCOPE emulator, are
9 summarized below and in Table 1.

Formatted: Subscript

10 2.3.4 TBM-SIF Models

11 Here we provide a brief description of individual TBM-SIF models and within model experiments.
12 We point out key differences in modeling of photosynthesis, fluorescence, and leaf-to-canopy
13 scaling. We note that within model experiments, labeled as Experiment 1 (exp1), Experiment 2
14 (exp2), etc, represent increasing order of realism, rather than a specific set of conditions common
15 across models. As such, Experiment 1 in BETHY (BETHY-exp1) is not equivalent to Experiment 1
16 in CLM4.5 (CLM4.5-exp1).

17 2.3.4.1 BETHY

18 The Biosphere Energy Transfer Hydrology (BETHY) model is the land surface component of the
19 Carbon Cycle Data Assimilation System (CCDAS) developed to ingest a range of observational data
20 for estimating terrestrial carbon fluxes at global scale (Rayner et al., 2005; Kaminski et al., 2013;
21 Koffi et al., 2012; Anav et al., 2015). Koffi et al. (2015) was the first to combine a process-based
22 model of SIF with a global TBM. The native canopy radiative transfer and photosynthesis schemes
23 of BETHY were effectively replaced with corresponding schemes and fluorescence model from
24 SCOPE (Koffi et al., 2015), thus enabling spatially explicit simulation of GPP and SIF as a function
25 of plant function type. This model was extended to include a module for prognostic leaf growth
26 (Norton et al., 2018) and more recently adapted with a formal optimization algorithm for
27 assimilating spaceborne SIF data (Norton et al., 2019). It has been updated for this study to accept
28 hourly meteorological forcing. BETHY-SCOPE, denoted here as BETHY, remains the first and only

Deleted: GPP

1 global TBM-SIF model to simulate vertically integrated (1-D) fluorescence radiative transfer and
2 energy balance.

3 We include three experiments to examine the impact of calibrating the k_N model against PAM
4 fluorometry data to different species: (1) *BETHY-exp1* is adapted to unstressed cotton species
5 (van der Tol et al., 2014), (2) *BETHY-exp2* is adapted to drought stressed Mediterranean species
6 (i.e., vineyard in controlled environment subjected to drought) including higher temperature
7 correction (Flexas et al., 2002; van der Tol et al., 2014), (3) *BETHY-exp3* is adapted to drought
8 stressed Mediterranean species (Flexas et al., 2002).

9 We further leverage SCOPE enabled SIF modeling in BETHY (*BETHY-exp3* specifically) to examine
10 (a) leaf and canopy level SIF and quenching under sunlit and shaded leaves, and (b) SIF emissions
11 at the top of canopy (SIF_{canopy}) versus the average emission within the canopy (SIF_{ave}), which
12 accounts for the average emission from sunlit and shaded leaves. The latter analysis facilitates
13 comparison to PhotoSpec, which observes the entire canopy.

14 An important caveat in the analysis of BETHY simulations is that, at the time of this writing, the
15 prescribed meteorological forcing at NR1 is only available for 2015. While this degrades
16 comparison to diurnal and synoptic variation observed by PhotoSpec in 2017, we find that
17 analysis of magnitude, light sensitivities, and within model experiments still provides useful
18 insight for interpretation of other TBM-SIFs, and future modeling requirements in general.

19 2.3.4.2 ORCHIDEE

20 The Organizing Carbon and Hydrology In Dynamic Ecosystems (ORCHIDEE) model (Krinner et al.,
21 2005) is the land surface component of the Earth System Model of Institut Pierre-Simon Laplace
22 IPSL-CM, (Dufresne et al., 2013) involved in recent exercises of the Coupled Model
23 Intercomparison Project (CMIP) established by the World Climate Research Programme
24 (<https://www.wcrp-climate.org/wgcm-cmip>). Recently a mechanistic SIF observation operator
25 was developed for ORCHIDEE to simulate the regulation of photosystem II ϕ_F at the leaf level
26 using a novel parameterization of NPQ as a function of temperature, PAR, and normalized ϕ_P . It
27 emulates the radiative transfer of SIF to the top of the canopy using a parametric simplification
28 of SCOPE. The details of the SIF modelling approach are provided in Bacour et al. (2019).

1 We include three experiments to examine the impact of water stress and parameter optimization
2 (using OCO-2 SIF, see Section 2.4): (1) *ORCHIDEE-exp1* is the standard configuration with default
3 parameters, (2) *ORCHIDEE-exp2* is the same as *ORCHIDEE-exp1* with two key differences (a) water
4 stress is applied to stomatal conductance, mesophyll conductance and to the photosynthetic
5 capacity, and (b) the tree height (12 m instead of 15 m) was set specifically for the NR1 site, (3)
6 *ORCHIDEE-exp3* is the same as *ORCHIDEE-exp1* but includes OCO-2 optimized parameters.

7 2.3.4.3 BEPS

8 The Boreal Ecosystem Product Simulator (BEPS) is an enzyme kinetic two-leaf model for
9 simulating carbon and water cycles for different plant functional types (Chen et al., 1999; Liu et
10 al., 2003). BEPS uses a modified Ball-Berry stomatal conductance model (Leuning et al., 1995)
11 and semi-analytical canopy radiative transfer. The canopy architecture is well considered in BEPS
12 model, which has not only remote-sensed LAI but also the global map of the foliage clumping
13 index. The fluorescence emission at the leaf level follows the approach of Lee et al (2015). SIF
14 emission for sunlit and shaded leaves are separately simulated based on illumination and canopy
15 geometry in BEPS. In addition, multiple scattering SIF is also simulated to account for the
16 scattering process within the canopy. The scaling of leaf-level fluorescence emission to the
17 canopy is based on a novel scheme for single-layer models which accounts for canopy scattering
18 and extinction from sunlit and shaded leaves (Qiu et al., 2019). This scaling scheme is an effective
19 approach to simulate the radiative transfer of SIF for a given canopy structure. We include two
20 experiments similar to *BETHY-exp1/2* in the calibration of the k_N model against unstressed vs
21 stressed species (*BEPS-exp1* and *BEPS-exp2*, respectively).

22 2.3.4.4 CLM4.5

23 The Community Land Model version 4.5 (CLM4.5) provides a description of the biogeochemical
24 profile spanning from the sub-surface bedrock to the top of the vegetation canopy. The
25 fluorescence sub-model follows Raczka et al. (2019), in which the degree of light saturation is
26 calculated from the potential and actual electron transport rate as determined from the
27 photosynthesis model described above. ϕ_f is formulated as described in Equation 2 and ϕ_p is
28 formulated as a function of the maximum ϕ_p under dark acclimated conditions and the degree

1 of light saturation. CLM4.5 uses independent site-level SCOPE simulations that match the
2 observed canopy characteristics and observed GPP at Niwot Ridge to calculate a leaf to canopy
3 level conversion factor (κ_{740}) for estimating SIF_{canopy} . In CLM4.5, κ_{740} is fitted to the modeled
4 SCOPE data as a function of solar zenith angle (and implicitly V_{cmax}).

5 Similar to Raczka et al. (2019), here we examine three separate approaches to parameterize k_N .
6 *CLM4.5-exp1* only considers reversible NPQ (k_R), such that, $k_N = k_R$, and the relationship
7 between k_R and the degree of light saturation is fitted to PAM fluorometry data based on
8 Mediterranean shrubs (Flexas et al., 2002; Galmes et al., 2007). *CLM4.5-exp2* parameterizes k_R
9 with PAM fluorometry from a Scots Pine forest (Porcar-Castell et al., 2011), and defines the rate
10 coefficient in terms of both a reversible and sustained component ($k_N = k_R + k_S$). It has been
11 found that sustained NPQ is important for cold climate evergreen conifer forests such as Niwot
12 Ridge (Miguez et al., 2015; Magney et al., 2019b), and Raczka et al. (2019) found that
13 representing both components provided improved simulations of seasonal SIF. *CLM4.5-exp3* is
14 similar to CLM4.5-exp3 but includes a seasonally varying representation of k_R . All model
15 experiments use hand-tuned parameters specific to US-NR1 (Raczka et al., 2016).

16 2.3.4.5 CLM5.0

17 CLM version 5.0 (CLM5.0) is similar to CLM4.5 with respect to the implementation of the
18 fluorescence sub-model, yet includes several important updates to the representation of
19 photosynthesis from CLM4.5, including a prognostic calculation of V_{cmax} based upon leaf nitrogen
20 and environmental conditions, revised nitrogen limitation scheme, Medlyn stomatal
21 conductance model, and plant hydraulic water stress (Kennedy et al., 2019). To represent NPQ
22 we use a single approach for k_N (see *CLM4.5-exp1*), but examine three approaches for estimating
23 κ_{740} : (1) *CLM5.0-exp1* uses κ_{740} as function of V_{cmax} following Lee et al (2015), (2) *CLM5.0-exp2*
24 follows the approach of *CLM4.5*, and (3) *CLM5.0-exp3* adapts the approach proposed by Zeng et
25 al. (2019) that estimates the fraction of total emitted SIF escaping the canopy by combining near-
26 infrared reflectance of vegetation (NIR_v) and fPAR.

27 2.3.4.6 SIB3

1 The Simple Biosphere Model version 3 (SIB3) involves the use of explicit biophysical mechanisms
2 to directly calculate carbon assimilation by photosynthesis (Baker et al., 2003; 2008). SIB3
3 includes prognostic calculation of temperature, moisture, and trace gases in the canopy air space,
4 but requires prescription of most structural properties including LAI. We examine two
5 approaches for prescribing LAI: (1) *SIB3-exp1* using values prescribed from MODIS, and (2) *SIB3-*
6 *exp2* uses values observed at the study site ($4.0 \text{ m}^2 \text{ m}^{-2}$). In general, the fluorescence sub-model
7 follows the approach of Lee et al. (2015) except that k_N is adapted to drought stressed species
8 following van der Tol et al (2014).

9 2.3.4.7 SIB4

10 SIB4 (Haynes et al., 2019a,b) shares many similarities to SIB3 with respect to functional aspects
11 of photosynthesis and fluorescence, however, SIB4 uses prognostic rather than prescribed
12 phenology and LAI.

13 2.3.5 SCOPE

14 SCOPE is a multi-layer canopy model which explicitly represents the within canopy radiative
15 transfer of fluorescence, whereas TBM-SIFs analyzed here (with the exception of BETHY) only
16 provide an empirical representation. We provide results from a stand-alone version of SCOPE
17 v1.73 (van der Tol et al., 2014) as an additional benchmark for TBM-SIF simulations of APAR, GPP,
18 SIF, and quantum yields. There are three important reasons for this: (1) It is inherently difficult
19 to provide representative and accurate *in situ* measurements of APAR, SIF, and GPP for
20 comparison to models; (2) SCOPE provides estimates of quantum yields for fluorescence,
21 photochemistry, and non-photochemical quenching, which are not measured continuously in the
22 canopy at NR1; and (3) SCOPE offers a more direct benchmark for evaluating more simplified
23 representations of canopy radiative transfer in TBM-SIFs. Unlike the TBM-SIFs, SCOPE does not
24 include a representation of biogeochemical cycling or carbon pools, and thus no spin up is
25 required. As such, we prescribe LAI ($4 \text{ m}^2 \text{ m}^{-2}$), canopy height (13 m), and leaf chlorophyll content
26 (25 ug cm^{-2}) following Raczka et al. (2019). We also examine two approaches for prescribing V_{cmax} :
27 (1) *SCOPE-exp1* uses the default constant value of 30, similar to *BETHY*, and (2) *SCOPE-exp2* uses
28 a seasonal varying value calibrated to NR1, following Raczka et al. (2016, 2019), which follows a

Formatted: Outline numbered + Level: 3 + Numbering
Style: 1, 2, 3, ... + Start at: 5 + Alignment: Left + Aligned
at: 0" + Indent at: 0.5"

1 [bimodal distribution peaking near 45 in early summer \(DOY = 150\) and 40 in late summer \(DOY =](#)
2 [250\)](#)

3 2.4 Data Assimilation

4 Details of the data assimilation protocols for [ORCHIDEE_{js}](#) provided in [Bacour et al. \(2019\)](#), [An](#)
5 ensemble of parameters related to photosynthesis (including optimal V_{cmax}) and phenology were
6 optimized for several plant functional types. Note that none of the assimilated pixels encompass
7 the location of the US-NR1 tower. [In](#) ORCHIDEE, the study site is treated as boreal needleleaf
8 evergreen (ENF); as such, the [ORCHIDEE-exp3](#) simulations in this study are based on parameters
9 optimized against OCO-2 SIF data using an ensemble of worldwide ENF pixels. Note that for
10 BETHY, each experiment uses the same set of optimized parameters whereas in ORCHIDEE the
11 SIF simulations are performed separately for the standard parameters ([ORCHIDEE-exp1/exp2](#))
12 and optimized parameters ([ORCHIDEE-exp3](#)), thus providing a test of sensitivity to parameter
13 optimization as discussed below.

14 2.5 Illumination Conditions

15 In order to gain insight into how SIF emissions and quantum yields vary with illumination, we
16 further analyze Photospec and a subset of models with respect to (a) changes in incoming light
17 and (b) self-shading within the canopy, respectively. For PhotoSpec, we analyze changes in
18 canopy average SIF and SIF_{rel} under conditions of predominantly direct versus diffuse PAR, using
19 [a](#) 0.5 threshold to distinguish between the two conditions (Section 2.2.3). For models we focus
20 on emissions from sunlit vs shaded leaves. We analyze leaf- versus canopy-level SIF emissions
21 (SIF_{leaf} and SIF_{canopy}) in [CLM4.5-exp3](#), and leaf-level quantum yields (ϕ_f , ϕ_p , ϕ_N) in [SCOPE-exp2](#).
22 We further compare predictions of quantum yield at the top-of-canopy to canopy averages in
23 [SCOPE-exp2](#). The motivation here is that top-of-canopy leaves see most of the sunlight, and thus
24 should have different yields compared to shade adapted leaves lower in the canopy. This also
25 provides a more direct comparison for PhotoSpec.

26 2.6 Modeling Protocol

27 Models are run for the period 2000-2018 (except BETHY [\(2015 only\)](#) and [SCOPE \(2017 only\)](#)) using
28 identical, hourly, gap-filled meteorological observations. The primary hourly output fields

Deleted: BETHY and

Deleted: are

Deleted: Norton et al. (2018) and

Deleted: , respectively

Deleted: For the two models,

Deleted: a

Deleted: Also, i

Deleted: the

Deleted: 2

Deleted: BETHY-exp3

Deleted: BETHY-exp3

Deleted: ,

1 analyzed are the top-of-canopy SIF (SIF_{canopy} @ 740 nm), GPP, ϕ_f , ϕ_p , and APAR. Model-
2 observation comparisons are made for absolute and relative SIF, GPP, SIF_{yield} ($SIF_{canopy}/APAR$) and
3 GPP_{yield} ($GPP/APAR$), sunlit versus shaded canopies (*CLM4.5-exp3* and *SCOPE-exp2*), and TOC
4 versus canopy average SIF (SIF_{canopy} versus SIF_{ave} , respectively, from *SCOPE-exp2*). Quantum yields
5 and within model experiments provide context to understand canopy integrated results. We
6 focus our analysis on 8 am – 4 pm local time from July-August 2017 for comparison to available
7 PhotoSpec and APAR data.

8 Models are controlled for meteorological forcing (meteorological data described in Burns et al.,
9 2015) but other factors such as spin-up, land surface characteristics, parameter tuning, and
10 model state, are not controlled for and are treated separately according to each model's
11 protocol. For example, CLM4.5 is better suited than others in prescribing observed vegetation
12 characteristics at the study site. One ORCHIDEE experiment (*ORCHIDEE-exp3*) is preliminary
13 optimized by assimilating independent Orbiting Carbon Observatory 2 (OCO-2) SIF data at the
14 global scale (Section 2.4). We emphasize that our point here is not to identify the best model but
15 to identify common patterns in model behavior through normalized SIF and deviation from
16 observed behavior to identify areas requiring the most attention.

17 The results are organized around two parallel themes. The first theme addresses four key
18 processes driving canopy-level fluorescence: (1) incoming illumination, (2) energy partitioning on
19 incoming light between photochemistry, fluorescence, and NPQ, and (3) leaf-to-canopy emitted
20 SIF, including linearity of yields at leaf and canopy scale. The second theme addresses sensitivity
21 of these processes to environmental conditions at diurnal and synoptic scales. Here, synoptic
22 scale refers to the impact of day-to-day changes in weather, including two storm events which
23 brought sustained cool, wet, and cloudy conditions from July 22-31 and then from August 6-10.

24 Section 3: Results

25 Incoming Illumination

26 Two key features dominate observed APAR variability: afternoon depression (Fig 2A) and
27 reduction during two summer storms (Fig 2D). Both features are captured by models. More
28 generally, models capture synoptic variability with high correlation ($r > 0.8$) and low across model

Deleted: BET

Deleted: HY

Deleted: 3

Deleted: BETHY

Deleted: 3

Deleted: Three BETHY experiment and o

Deleted: were

1 spread ($\sigma = 10\%$). The exception is BETHY, which is simulated outside our observation year (2015).
2 High model fidelity is expected given that observed PAR is prescribed, and it is promising that
3 models show a consistent response to changes in illumination. The primary shortcoming across
4 TBM-SIFs and SCOPE is a systematic high bias in APAR magnitude (129%), with most models
5 exceeding the upper range of observed APAR (as determined from the six within canopy PAR
6 sensors, Fig S2), and high model spread. These errors are likely related to differences in predicted
7 fAPAR. In the case of ORCHIDEE, high APAR is expected due to the big leaf assumption where all
8 leaves are considered as opaque and fully absorbing.

9 *Canopy Photosynthesis*

10 Observed GPP shows a broad peak from mid-morning to early afternoon (~9 am – 1 pm local),
11 followed by slight decrease until 4 pm (Fig 2B), consistent with afternoon cooling and reduced
12 light availability (Fig 1B-D). The two month period under investigation is relatively flat with
13 generally weak day-to-day variability ($\sigma = 17\%$), but modest correlation with APAR ($r = 0.61$, Fig
14 2E). Some models capture the afternoon GPP depression, but all models strongly underestimate
15 its magnitude, apparently independent of stomatal conductance formulation or more explicit
16 accounting for plant hydraulic water stress such as in CLM5.0. SCOPE and BETHY, which don't
17 account for water stress, show no afternoon depression. Models are mostly uncorrelated with
18 observed GPP at synoptic scale (r ranges from -0.2 to 0.36, highest value in SiB4), high biased,
19 and show increased spread (in predicted magnitude) relative to APAR (143% +/- 23%). SCOPE-
20 exp2 shows slight improvement in GPP magnitude with the larger V_{cmax} value in late summer.

21 While observed GPP_{yield} is mostly stable over the diurnal cycle, most models (except BEPS) show
22 a distinct midday minimum (Fig 3A). Half of the models show a similar midday minimum in
23 photochemical quantum yield (ϕ_p , Fig 4A), with the other half either increasing or decreasing in
24 the afternoon (CLM5.0 and SiB3/SiB4, respectively). The midday dip in yield is likely associated
25 with reduced photosynthetic efficiency at high light levels, as demonstrated by reductions in GPP,
26 GPP_{yield} , ϕ_p with APAR (Fig 5A, C, E).

27 Observed GPP_{yield} shows significant structure at synoptic temporal scale (Fig 3C), most notably
28 increased yield during the cool/rainy period (reduced heat and water stress), and decreased yield

Deleted: s

1 in mid- to late- August (increased heat and water stress following the cooling pattern). In contrast
2 to predicted GPP, models show high fidelity in capturing the magnitude and variability of GPP_{yield}
3 at synoptic scale (r ranges from 0.35 – 0.76, highest values in *SCOPE* and *CLM4.5/5.0*). Individual
4 models are self-consistent in their predictions of GPP_{yield} and ϕ_P at synoptic scale ($r = 0.592$ –
5 0.935) except for SiB3/SiB4 ($r < 0.1$, Fig 4B).

6 *Canopy Fluorescence*

7 Observed SIF_{canopy} is strongly correlated with observed APAR at diurnal and synoptic scale ($r =$
8 0.77), with common features including afternoon depression and reduction during rainy periods
9 (Fig 2C & 2F). Observed PAR also feeds into the fluorescence sub-model and, unlike GPP, strongly
10 correlates with SIF_{canopy} at synoptic scale (r ranges from 0.58 to 0.92, highest values in *SCOPE* and
11 *ORCHIDEE*). However, we find a persistent positive model bias in SIF_{canopy} (170% +/- 45%)
12 consistent with, but not proportional in magnitude to, the APAR bias. We note that models are
13 especially oversensitive to APAR at high light levels (Fig 5D).

14 We investigate the high bias in SIF_{canopy} in more detail using *SCOPE-exp2* and *CLM4.5-exp3*.
15 Specifically, we examine leaf and canopy level SIF and quenching under sunlit and shaded leaves.
16 Analysis of quantum yields in *SCOPE-exp2* (Fig S5) shows a reversal in the fractional amounts of
17 absorbed energy going to SIF and PQ vs NPQ in low- vs high-light conditions that is consistent
18 with leaf level data and theory (Porcar-Castell et al., 2014). More specifically, *SCOPE-exp2*
19 predicts low ϕ_F and ϕ_P and high ϕ_N in sunlit leaves relative to shaded leaves, with more energy
20 going to fluorescence and photochemistry than to NPQ in shaded leaves, and more energy going
21 to (shed off by) NPQ in sunlit leaves (Fig S5). Likewise, total ϕ_F shows decreasing values with
22 increasing APAR in *SCOPE* and *BETHY-exp2/3* compared to *BETHY-exp1*, consistent with observed
23 SIF_{yield} (Fig 5E-F), as ϕ_N ramps up to higher levels in the drought parameterized Kn model.
24 Moreover, in stark contrast to SIF_{yield} and SIF_{canopy} , ϕ_F does not show high values relative to other
25 models (Fig 4D). These results point to an issue in *SCOPE* and *BETHY* with leaf to canopy scaling
26 in needleleaf forests.

27 Analysis of *CLM4.5-exp3* suggests several possible reasons for oversensitivity to APAR. First, we
28 focus on emissions from sunlit/shaded portions of the canopy (Fig S6). *CLM4.5-exp3* and

Deleted: BETHY

Deleted: 3

Deleted: BETHY-exp3

Deleted: BETHY-exp3

Deleted: BETHY

Formatted: Not Highlight

1 PhotoSpec both show higher SIF under “high light” conditions (sunlit leaves and direct radiation,
2 respectively) compared to “low light” conditions (shaded leaves and diffuse radiation,
3 respectively), which is promising (Fig S6 A,D). Comparing the ratio of sunlit to shaded SIF in
4 *CLM4.5-exp3* to the ratio of direct to diffuse SIF in PhotoSpec (Fig S6 B,E) shows higher ratio in
5 *CLM4.5-exp3* on average. The difference peaks in midday, when sunlit leaf area is maximized
6 (self-shading minimized) in CLM4.5 but no major difference in the amount of direct radiation,
7 and decreases with increasing sun angle (morning and afternoon) and with increasing rainfall (in
8 the afternoon on average, and during the rainy period in late July / early August), both of which
9 increase the shaded fraction. As such, accounting for view angle and different illumination
10 metrics for PhotoSpec and CLM4.5 (most comparable in morning, afternoon, and during rainy
11 days) reduces, but does not entirely remove, the positive bias in high light conditions.

12 Second, the degree of light saturation (x) is twice as high in the sunlit canopy in *CLM4.5* (Fig S7),
13 which leads to low fluorescence efficiency in sunlit leaves and high fluorescence efficiency in
14 shaded leaves. While this produces high photochemistry in shaded leaves, it contributes a small
15 fraction of SIF to the total canopy (~20%) despite higher fractions of shaded leaves (~2/3 at noon,
16 Fig S6C) and thus sunlit leaves dominate SIF_{yield} and SIF_{canopy} . Therefore, it seems likely that a
17 model’s representation of canopy structure including the partitioning between sunlit/shaded leaf
18 area fractions has an important impact upon canopy SIF. Biases in the sunlit/shaded fraction will
19 likely propagate into the simulated value of canopy SIF. However, it’s important to know that the
20 observed sunlit/shaded fraction from PhotoSpec is estimated as well, since it is currently not
21 possible to determine the precise sun/shade fraction within PhotoSpec FOV.

22 Additionally, all formulations of CLM4.5 (and most models except BETHY and SCOPE) show lack
23 of decline in SIF_{yield} with APAR compared to measurements of absolute SIF (Fig 5E). For CLM4.5,
24 the relationship between SIF_{yield} and APAR depends upon the relationship between degree of
25 light saturation and reversible NPQ (Raczka et al., 2019). This suggests it is important to properly
26 represent the NPQ response to environmental conditions when simulating $SIF_{}$.

27 While most of the model bias is reduced in SIF_{yield} (126%, mostly attributed to BETHY and SCOPE),
28 the remaining signal, representing the dynamic response to synoptic conditions (e.g., Magney et
29 al., 2019), is poorly represented in models, as demonstrated in a time series of 5-day means (Fig

Deleted: , fraction of absorbed light not used in photosynthesis...

Deleted: high

Deleted: low

Deleted: canopy

1 3D). Most models show zero to strongly negative correlation with observations at synoptic scale
2 and only three models (SCOPE, ORCHIDEE-exp3, and BETHY-exp2/3), produce correlation greater
3 than 0.5. These are the only three models that also capture a negative relationship between
4 SIF_{yield} and APAR (Fig 5E).

Deleted: two

Deleted: CLM4.5

Deleted: positive

5 In general, predicted SIF_{yield} is stable during our short study period (Fig 3). Half of models show a
6 significant positive correlation with GPP_{yield} (r > 0.85) and half show zero or negative correlation
7 (Fig S8). While these findings run counter to observed SIF_{yield}, which shows a clear response
8 during and following the storm event and moderate positive correlation with observed GPP_{yield} (r
9 = 0.40), they show some consistency with observed SIF_{rel} (grey line in Fig 3 and Fig S8A) which
10 like many models is stable and uncorrelated with GPP_{yield}. We refer the reader to Section 2.2.2
11 for clarification of the important difference between SIF_{yield} and SIF_{rel}.

Deleted: ations of

Deleted: most

Deleted: predictions

12 Leaf-to-Canopy Scaling

Deleted: here, since these metrics represent different but equally important versions of reality. SIF_{yield}, estimated as the ratio between absolute canopy SIF (SIF_{canopy}) and APAR, is our best attempt to account for the effect of canopy absorbed light on the canopy integrated emission of SIF. However, factors such as observation angle, sunlit bias, and difference in footprint from APAR, necessitates our alternative calculation in SIF_{rel}. While SIF_{rel} removes model-observations differences in illumination, it confounds our interpretation of the relationship with GPP_{yield}, which is derived from APAR. As such, we provide both results to be comprehensive, but note the temporal stability associated with SIF_{rel} as the more physical interpretation of canopy yield for this short period of study. ¶

13 Several methods have been proposed to transfer predicted leaf-level SIF emissions to the top of
14 canopy. While leaf-to-canopy scaling enables efficient global scale simulation, the diversity of
15 novel methods adds uncertainty to the canopy level estimate of SIF (in addition to
16 aforementioned uncertainties in structure, APAR, photochemistry, fluorescence). These
17 differences are evident in comparison of Figures 3 and 4, in which yields are plotted on a similar
18 scale.

19 At least at diurnal scale, there is some evidence that leaf and canopy emissions look more similar
20 for models adopting simplified empirical scaling functions (SiB3, SiB4, CLM4.5, CLM5.0, BEPS)
21 than for models that more explicitly account for radiative transfer (SCOPE, BETHY, ORCHIDEE).
22 For the more explicit models, the diurnal cycle of ϕ_f is out of phase with SIF_{yield}, the former of
23 which peaks in the afternoon and the latter of which peaks in the morning. This produces
24 reasonable agreement to PhotoSpec in phase and magnitude between SIF_{yield} and SIF_{rel} for
25 ORCHIDEE, but produces divergence in the magnitude of SIF_{canopy} for ORCHIDEE.

Deleted: yield

26 Model performance in leaf-to-canopy scaling is summarized in Figure S8. The only three models
27 with a positive relationship between yields (Fig S8B) and between quenching terms (Fig S8C)
28 include explicit representation of radiative transfer (i.e., SCOPE, BETHY, and ORCHIDEE). CLM4.5

Deleted: two

Deleted: are the two models with more

1 is the only model with a positive relationship between yields, but not between quenching terms.
2 SiB3/SiB4 are the only models with a positive relationship between quenching terms, but not
3 between yields.

4 Finally, we clarify an important difference between observed and predicted estimates of canopy
5 average SIF. PhotoSpec scans direct emissions from sunlit and shaded leaves within the canopy,
6 thus observing the ‘total’ emission from leaves in the instrument FOV. We then average each of
7 these leaf-level scans and report as canopy averages. Model output, in contrast, is reported at
8 the TOC, which represents the ‘net’ emission from leaves after attenuation in the canopy
9 (through canopy radiative transfer, re-absorption of SIF, and shading). Assuming sunlit and
10 shaded leaves within the canopy emit at the same rate as TOC leaves, attenuation will reduce the
11 effective signal from leaf-level emissions within the canopy. As such, the average of leaf level
12 emissions (canopy average) is expected to be lower than the net emission of leaves reaching the
13 top of canopy.

14 This is important because CLM4.5, shows strong attenuation of SIF from leaf-level to TOC,
15 decreasing by a factor of 2-3 at midday (Fig S7). The interpretation here is that the model bias in
16 absolute SIF may actually be higher than reported here; however, we note that more quantitative
17 information on the observed fraction of sunlit vs shaded leaves and comparative top-of-canopy
18 SIF values for the same canopy elements are needed (to account for off-nadir SIF viewing) for
19 more accurate determination of scaling between observed canopy and top-of-canopy SIF.

20 *Within Model Experiments*

21 In most cases, within model experiments produce improvements in some metrics and
22 degradation across others (performance change is quantified by reporting correlation values in
23 brackets). An important and unexpected result of this study is the impact of different levels of
24 tuning to observations on our predictions. While this work represents a snapshot of the state-of-
25 the-art in site-level TBM-SIF modeling, and we have taken great care to control for environmental
26 conditions (most important being illumination), an important overall takeaway is for future
27 model comparisons to make additional efforts to control for initial conditions and vegetation
28 state (i.e. model biophysical parameters).

Deleted: ¶
Deleted: Finally, we note that PhotoSpec scans of leaf-level emissions are averaged and reported here as canopy averages, while model output is reported at the top of the canopy, which accounts for within-canopy radiative transfer, re-absorption of SIF, and shaded canopies, causing lower emissions compared to the canopy average.
Deleted: , for example,

1 The most basic example is tuning of LAI in SiB3 [and \$V_{cmax}\$ in SCOPE](#). LAI, as prescribed by MODIS
2 for *SiB3-exp1* (~1.5), is on the low end for a subalpine evergreen forest, and consequently
3 produces negative biases in APAR, GPP, SIF and SIF_{yield}. When prescribed according to tower
4 observations in *SiB3-exp2* (~4.0), the biases become positive (albeit on the lower end of the
5 model ensemble), but produces degraded variation at synoptic scale for GPP (0.39 vs 0.19), SIF
6 (0.87 vs .71) and SIF_{yield} (0.09 vs -0.32). [The tuning of \$V_{cmax}\$ in SCOPE improves the magnitude of](#)
7 [GPP, with minimal impact on variability at diurnal- to synoptic- scale.](#)

8 Experiments in CLM4.5 comprise a higher level of hand tuning of vegetation structural and
9 functional characteristics. Parameter tuning was imposed to match vegetation structure with
10 site level measurements and consequently CLM4.5 produces overall low bias in yields. With
11 respect to synoptic variation, NPQ experiments, tuned against the measured air temperature and
12 a representative evergreen forest, produce improvements at synoptic scale for GPP (-0.01 vs
13 0.16), SIF (0.59 vs 0.86), and GPP_{yield} (0.05 vs 0.63), but degradation in SIF_{yield} (0.32 vs -0.25).
14 Likewise, NPQ experiments in BETHY based on species information (calibration of K_N against PAM
15 fluorescence in stressed vs unstressed systems) shows improvement in the SIF_{yield}-APAR
16 relationship for drought stressed models (*BETHY-exp1* vs *BETHY-exp2/3*).

17 Experiments with ORCHIDEE demonstrate that errors in model parameters (such as V_{cmax} , LAI_{max},
18 leaf age, or SLA) contribute to SIF and GPP uncertainty but can be alleviated by assimilation of
19 OCO-2 SIF retrievals (*ORCH-exp1/2* vs *ORCH-exp3*). Model optimization of parameters improves
20 the functional link between SIF and GPP, thus reducing biases in APAR, GPP, and SIF_{yield}, and
21 improving synoptic variation in SIF_{yield} (-0.04 vs 0.58).

22 **Section 4. Discussion**

23 This study represents a first attempt to evaluate a controlled ensemble of TBM-SIF models
24 against canopy integrated SIF observations to identify and attribute model-observation
25 mismatches related to errors in canopy absorption of sunlight, photosynthesis, fluorescence, and
26 leaf-to-canopy radiative transfer of fluorescence.

27 Different models match some observed parameters better than others (with respect to APAR and
28 yield), but no model gets both APAR and SIF_{yield} magnitude and/or sensitivities close to the

1 observations. For example, BEPS closely matches the magnitude of APAR (Fig 2A), and BETHY
2 captures the decline in SIF_{yield} with APAR for NPQ quenching based on stressed species (Fig 5E),
3 but both models overestimate observed yield by a factor of 2, hence SIF is overestimated (Fig 2).
4 CLM4.5 correctly captures the diurnal SIF_{yield} change, but overestimate APAR; in this case, SIF and
5 SIF_{yield} are overestimated. Importantly, models diverge strongly from each other and from
6 observations in the magnitude of SIF_{yield} and its decline with APAR (Fig 5E), partially reflecting
7 model variability in ϕ_f (Fig 5F), but in general show a characteristic pattern of weak SIF_{yield} decline
8 with APAR. GPP_{yield} shows higher agreement between models and with observations (Fig 5B),
9 despite divergent ϕ_p (Fig 5C), which could be indication that the primary uncertainty is due to
10 the representation of fluorescence and not the photosynthesis model.

11 Consequently, we find a strong linear and positive relationship between observed SIF_{yield} and
12 GPP_{yield} for absolute SIF, which is underestimated on average by models (Fig S8A-B). In contrast,
13 models show quite strong positive relationships between ϕ_f and ϕ_p (Fig S8C). Our study
14 highlights an apparent challenge for models in transferring leaf level processes to canopy scale,
15 and consequently, linking the proper canopy mechanistic SIF-GPP relationship at the leaf level.

16 The mismatch between multi-model simulations and tower-based observations of SIF and GPP
17 at hourly and daily scales can be summarized as symptoms of five main factors: (1) PhotoSpec
18 scan strategy, (2) radiative transfer of incoming PAR and impact on APAR and sunlit/shaded
19 fraction, (3) representation of photosynthesis and sensitivity to water limitation especially during
20 afternoon conditions, (4) representation of fluorescence and sensitivity to reversible NPQ
21 response at Niwot Ridge, and (5) radiative transfer of fluorescence from leaf to canopy. Several
22 persistent biases falling under these broad categories are discussed below.

23 **Apples to Apples Comparison.**

24 PhotoSpec is unique in its ability to scan entire canopies for signals that are largely hidden from
25 nadir-oriented instruments. However, this creates unique challenges for interpretation of data
26 and comparison to models. For example, the diurnal cycle of observed SIF is highly sensitive to
27 view angle. PhotoSpec was set up in 2017 to scan back-and-forth between northwest and
28 northeast view angles, but the instrument was slightly biased to the northwest, causing a low

Deleted: 6

Deleted: 6

1 phase angle in the morning (more aligned with rising sun) and increased phase angle in the
2 afternoon (more opposed to setting sun). As such, PhotoSpec observed predominantly
3 illuminated canopies in the morning and shaded canopies in the afternoon (i.e., more shaded
4 fraction), leading to the late morning peak in reflected radiance (Fig S3).

5 Moreover, Photospec scans specific locations at the top of the canopy from near nadir to view
6 angles closer to the horizon (see Fig. S8 in Magney et al., 2019b), while models are currently
7 configured to simulate top of canopy emission and simulated here as nadir viewing. The question
8 becomes whether to retain nadir only data and sacrifice signal-to-noise, or to average over all
9 elevation angles and risk aliasing view angle effects. This study, partly motivated by high
10 agreement of canopy integrated SIF with spaceborne data from OCO-2 and TROPOMI (Magney
11 et al., 2019b; Parazoo et al., 2019), has chosen the latter approach but with an attempt to
12 minimize scan angle effects in SIF_{rel} . However, it is worth noting that swath sensors such as
13 GOME-2 show high sensitivity to viewing angle especially under increasing illumination angles
14 (Kohler et al., 2018; Joiner et al., in review). View angle effects are likely to be especially acute
15 for PhotoSpec in the morning and afternoon with increasing anisotropy and changes in the
16 illuminated field of view with sun and view angle. Other tower SIF instruments with a wide FOV
17 (i.e. FluoSpec2; Yang et al., 2018) may more appropriately represent the TOC SIF emission, but
18 also have difficulty disentangling the sunlit/shaded canopy components.

19 It is critical that model evaluation relative to measured SIF data and data assimilation studies
20 properly account for the specificities of the instrument (viewing of the instrument, spectral band,
21 time of the overpass for space-borne instruments), the representation of canopy emission, and
22 correct observations for directional variations in SIF relative to observation geometry. Although
23 normalizing SIF by reflected radiance partially alleviates scan angle effects, this highlights the
24 need for models to get canopy structure, radiative transfer, and sunlit/shaded fraction correct,
25 which feed all the way through to SIF and GPP. Further ground-based investigations of SIF
26 anisotropy, sunlit/shade fraction, and vertical distribution (within canopy, canopy integrated,
27 and top of canopy) with PhotoSpec [and SCOPE](#) may help to inform models on the physical aspects
28 of the signal. Despite the issues we highlight in comparing observations to models, the potentially

1 more interesting and important story here is with respect to model-model comparisons, which
2 reveals wide divergence in response to light conditions and other factors, as discussed below.

3 **TBM SIF is too sensitive to APAR.**

4 Our results indicate a wide range of SIF responses to APAR: TBM-SIFs and SCOPE are usually far
5 too sensitive to APAR, observations of absolute SIF are less sensitive, and observations of relative
6 SIF (SIF_{rel}) are least sensitive (Fig. 5D). We remind the reader that SIF_{rel} is normalized by the
7 amount of far-red light reflected from leaves in the FOV of PhotoSpec, and thus has reduced
8 sensitivity to absorbed light than absolute SIF. The fact that SIF_{rel} is the least sensitive to APAR
9 means other processes are driving changes in SIF under increased light absorption. In this case,
10 it reveals a strong SIF response to changes in photochemical quenching. SIF models appear
11 especially sensitive to sunlit leaves. In CLM4.5, SIF emissions from the sunlit portion of the canopy
12 are a factor of 5 higher than emissions from shaded leaves, despite twice as fewer leaves in the
13 sunlit canopy (Fig S6C). In CLM4.5, the combination of higher than average ϕ_f (Fig 5F) with higher
14 fluorescence efficiency in the sunlit portion of the canopy, produce an increase in the magnitude
15 and sensitivity to sunlit fraction, thus contributing to the high bias (factor of 3 higher than
16 observed) and strong diurnal cycle (2-fold increase from morning to midday).

17 **Linearity of SIF and GPP yields.**

18 Observations show a positive but not significant linear relationship between SIF_{yield} and GPP_{yield}
19 (Fig 6A, $r = 0.40$) at our study site. This is likely due to the short time period investigated here
20 where there is relatively little change in SIF_{yield} and GPP_{yield} during peak summer. Half of models
21 (4 of 8) show a significant ($r > 0.35$) linear and positive slope ($r > 0.35$; SCOPE, ORCH-exp3,
22 CLM4.5-exp3, and BETHY-exp3) between SIF_{yield} and GPP_{yield} , while 6 models (except CLM5.0)
23 show a significant positive slope between quantum yields (ϕ_f and ϕ_p , Fig S8C). These regression
24 plots of quantum yields, in turn, help explain the observed linearity of SIF_{yield} vs. GPP_{yield} : At least
25 in the case of Niwot Ridge, model (and presumably observed) ϕ_p stays within high light “NPQ-
26 Phase” conditions, and generally doesn’t exceed the range in which decoupling of ϕ_f and ϕ_p (ϕ_p
27 > 0.6) in low light “PQ-Phase’ conditions occurs (Porcar-Castell et al., 2014, cf Fig 9). SCOPE and
28 BETHY-exp3, which best capture the observed relationship in the canopy between SIF_{yield} and

Deleted: spectrum

Deleted: .

Deleted: The fact that relative SIF is the least sensitive is telling, as it reduces sensitivity to APAR and reveals a strong SIF response to changes in photochemical quenching.

Deleted: Only 3 of 7

Deleted: 5

Deleted: 6

Deleted: s

Deleted: is

Deleted: is

1 GPP_{yield}, are also the only models that also shows a decline in SIF_{yield} with APAR, as discussed
2 below. These results are likely to change when we expand the study to several years; however,
3 the purpose of this study was to provide an initial investigation into the response of modelled SIF
4 and GPP to light during peak summer.

5 **Insufficient decline in SIF_{yield} with APAR.**

6 In general, models show an insufficient decline in SIF_{yield} with APAR, when compared to observed
7 SIF_{yield} (Fig 5E). All models except SiB3 and SiB4 show some decline, with BETHY showing the best
8 agreement in slope magnitude. SCOPE and BETHY are the only models with full radiative transfer
9 but this does not appear to have a substantial impact on SIF_{yield}, which has a similar (albeit
10 suppressed) decline with APAR as ϕ_f (Fig 5F). Within model experiments show little to no
11 sensitivity of SIF_{yield} or ϕ_f decline with APAR to water stress (e.g., ORCHIDEE) or prescribed LAI
12 (e.g., SiB3), but high sensitivity to the formulation of NPQ with respect to species calibration (e.g.,
13 BETHY) and reversibility (e.g., CLM4.5).

14 Three CLM4.5 experiments demonstrate sensitivity to representation of NPQ variability at diurnal
15 and seasonal scales. The first simulation using the default NPQ parameterization from SCOPE
16 (*CLM4.5-exp1*, based on a 2-parameter fit to drought stressed Mediterranean species (Galmes et
17 al., 2007) produces the strongest decline in SIF_{yield}. The second simulation, which includes a site-
18 specific NPQ formulation that accounts for k_R and k_S (*CLM4.5-exp2*), produces the weakest
19 decline. The third simulation with seasonally varying k_R produces a slightly stronger decline. An
20 important point for this formulation is that k_R is constrained by PAM fluorometry data at Hyytiala
21 (Scot Pine) and does not account for high light saturation values and summer drought conditions
22 that may be more typical of lower latitude sites such as Niwot Ridge. This could indicate that
23 parameterizing k_R based upon similar PFTs may not be sufficient to properly characterize the NPQ
24 response for lower latitude sites such as Niwot Ridge.

25 Similar results are found in experiments with BETHY comparing stressed (drought) and
26 unstressed (relative to water availability) NPQ models at NR1 but controlling for k_R (constant in
27 time in both cases, stronger negative SIF_{yield} response to APAR in stressed model). In the
28 unstressed models of CLM4.5 and BETHY, the NPQ response to APAR becomes too low, causing

1 an oversensitivity of SIF to APAR and thus high SIF bias. The strongly regulated NPQ response of
2 the drought-based model enables more non-photochemical quenching at high light levels in
3 stressed ecosystems compared to typical unstressed plants. While this k_{NPQ} model was
4 developed using drought-stressed plants, similar up-regulation of NPQ is expected to occur under
5 any condition where photosynthesis is limited and available excitation energy is high (e.g. cold
6 temperatures and high light, Sveshnikov et al., 2006). Our results thus emphasize the need for
7 careful implementation of NPQ dynamics for simulating and assimilating SIF in different light and
8 stress environments (Raczka et al., 2019; Norton et al., 2019).

Deleted: , doi: [10.1093/treephys/26.3.325](https://doi.org/10.1093/treephys/26.3.325)

9 **Data assimilation reduces high bias.** Assimilation of OCO-2 SIF in ORCHIDEE brings the magnitude
10 of both GPP and SIF in closer agreement with observations. This improvement is driven by
11 decreases in leaf photosynthetic capacity (V_{cmax} , LAI_{max} , leaf age, SLA, Bacour et al., 2019), which
12 decreases the magnitude (but not shape) of APAR closer to observed values (Fig 2), and leads to
13 improvements in GPP_{yield} and SIF_{yield} (Fig 3). Nevertheless, after the assimilation there are still
14 disagreements in SIF_{yield} vs GPP_{yield} relative to the measured quantities (Fig S8). For diurnal and
15 synoptic cycles, the assimilation effectively acts to scale the magnitude of SIF, GPP and APAR (and
16 related yields), but it does little to alter variability. Although data assimilation (i.e. calibrating
17 model parameters) is critical to improving modelled SIF and GPP, this should be done in
18 conjunction with improvements in the model formulation (as summarized in Section 5),
19 otherwise the estimated model parameters can be sub-optimal to compensate for the lack of
20 missing processes.

Formatted: Subscript

Formatted: Subscript

Deleted: 6

21 **5. Conclusions/Recommendations**

22 Our results reveal systematic biases across TBM-SIF models affecting leaf-to-canopy simulations
23 of APAR, GPP, and SIF. This highlights key areas where observing strategies and model
24 formulations can be improved:

- 25 1) Radiative transfer of incoming and absorbed PAR. The representation of incoming radiative
26 transfer produces positive biases in APAR that leads to positive biases in GPP, both of which
27 occur regardless of time of day. This is influenced by characterization of the canopy, leaf
28 orientation and clumping, biochemical content, canopy layers, and leaf area, which dictates

1 the sunlit/shaded fractions of the canopy. Furthermore, the combination of high APAR bias
2 in models and high uncertainty in observed APAR highlights a need for more accurate and
3 representative *in situ* measurements of APAR within the FOV of SIF observations and
4 footprint of eddy covariance data. We recommend further site-level investigation of
5 observed and simulated canopy light absorption, emphasizing comparison of multi-layer and
6 multi-leaf radiation schemes accounting for sunlit and shaded leaf area.

Formatted: Font: Italic

7 2) Water stress impacts on photosynthesis. The underlying photosynthetic models fail to
8 simulate the magnitude of depression of observed GPP in the afternoon, regardless of how
9 stomatal-conductance and water stress models and parameters are formulated. This likely
10 results from the inability to account for afternoon water stress to properly restrict stomatal
11 conductance and hence GPP and SIF. Additional effort is needed to characterize SIF and GPP
12 sensitivity to increased atmospheric demand and/or reduced soil moisture across a range of
13 managed and unmanaged systems. We also recommend more inclusion of stomatal
14 optimization models (e.g., Eller et al., 2020) as optional parameterizations for TBMs, to better
15 account for plant hydraulic functioning under water stress compared to the more widely used
16 semi-empirical models.

Deleted:

Deleted: or

Deleted: formulation

17 3) Leaf Mechanism for Energy Partitioning. We provide evidence that many models fail to
18 capture the correct reversible NPQ response to light saturation, leading to biases in SIF_{yield}
19 during high light conditions and especially with increasing moisture limitation at the end of
20 summer. Further investigation using models such as BETHY and CLM is needed to better
21 characterize sensitivity of NPQ formulations to PFT and environmental conditions. We also
22 emphasize a need for more simultaneous measurements of active and passive chlorophyll
23 fluorescence to determine the temporal dynamics of competing pathways (PQ, NPQ) from a
24 wider variety of plant species under ambient conditions and different levels of stress.

25 4) Radiative transfer of SIF. SIF is emitted from the leaf level (sunlit shaded fractions of leaf level)
26 and then is transferred to the top of canopy as a function of canopy structure (leaf geometry,
27 canopy layers, leaf area). Despite high disagreement of SCOPE and BETHY with respect to the
28 simulation of APAR and SIF magnitude, we recommend site level simulations using a similar

Deleted: -SCOPE

1 framework where a radiative transfer model is run both offline and coupled to a terrestrial
2 biosphere model for more detailed investigation of sensitivity to canopy characteristics.

3 5) Observation strategy. The PhotoSpec scan strategy enables direct measurement of SIF
4 emission at leaf-to-canopy scale, but requires off-nadir view angles that lead to changing
5 fractions of sunlit and shaded canopies throughout the day as a function of sun angle. Further
6 work could be done using tower mounted instruments with a wider FOV that more accurately
7 represent top of canopy emissions for comparison to model simulations, and to classify
8 emissions from shaded vs sunlit canopies. More effort is also needed to better align models
9 with observations, for example by leveraging three-dimensional capabilities in SCOPE (and
10 other RTMs) to directly account for multiple observation angles.

11 6) Finally, we note that our focus on a water limited subalpine evergreen needleleaf forest
12 represents a challenging case study for models and observations. In many cases, there is
13 strong covariance between LAI, SIF, APAR and GPP in cropping systems (Dechant et al., 2020),
14 but because this study site experiences little change in canopy structure and APAR
15 throughout the season (Magney et al, 2019b), our study sought to provide more explicit
16 insight into the models sensitivity to photosynthesis and fluorescence. As such, it is possible
17 that we would see more convergence of results, and a reduction in confounding effects (e.g.,
18 decreased NPQ), in a well-watered high-LAI cropping system. We therefore recommend
19 similar model-observation assessments across a wider range of biota and climate.

20 **Acknowledgements**

21 The US-NR1 AmeriFlux site is supported by the U.S. DOE, Office of Science through the AmeriFlux
22 Management Project (AMP) at Lawrence Berkeley National Laboratory under Award Number
23 7094866. BMR was supported by the NASA CMS Project (award NNX16AP33G) and the US
24 Department of Energy's Office of Science, Terrestrial Ecosystem Science Program (awards DE-
25 SC0010624 and DE-SC0010625). CESM (CLM4.5 and CLM5.0) is sponsored by the National
26 Science Foundation and the U.S. Department of Energy. ORCHIDEE is supported by CNES-
27 TOSCA under the FluOR and ECOFLUO projects. ITB was supported by NASA contract
28 80NSSC18K1312. We would like to thank the W.M. Keck Institute for Space Studies and internal

1 funds from the Jet Propulsion Laboratory for support of the field measurements at Niwot Ridge
2 (<http://www.kiss.caltech.edu/study/photosynthesis/technology.html>). A portion of this research
3 was carried out at [the Jet Propulsion Laboratory](#), California Institute of Technology, under
4 contract with NASA. This work was supported in part by the NASA Earth Science Division
5 MEaSURES program (grant 17-MEASURES-0032) and ABoVE program (18-TE18-0062). Copyright
6 2019. All rights reserved.
7

Deleted: JPL

1 **References**

- 2 [Aasen, H., Van Wittenbergh, S., Medina, N. S., Damm, A., Goulas, Y., Wieneke, S., Hueni, A.,](#)
3 [Malenovsky, Z., Alonso, L., Pacheco-Labrador, J., and Cendrero-Mateo, M.P.: Sun-induced](#)
4 [chlorophyll fluorescence II: Review of passive measurement setups, protocols, and their](#)
5 [application at the leaf to canopy level. *Remote Sensing*, 11\(8\), p.927, 2019.](#)
- 6 Anav, A., Friedlingstein, P., Beer, C., Ciais, P., Harper, A., Jones, C., Murray-Tortarola, G., Papale,
7 D., Parazoo, N.C., Peylin, P., and Piao, S.: Spatiotemporal patterns of terrestrial gross
8 primary production: A review, *Reviews of Geophysics*, 53(3), 785-818,
9 <https://doi.org/10.1002/2015RG000483>, 2015.
- 10 Albert, L. P., Keenan, T. F., Burns, S. P., Huxman, T. E., and Monson, R. K.: Climate controls over
11 ecosystem metabolism: insights from a fifteen-year inductive artificial neural network
12 synthesis for a subalpine forest, *Oecologia*, 184(1), 25–41.
13 <https://doi.org/10.1007/s00442-017-3853-0>, 2017
- 14 Bacour, C., Maignan, F., MacBean, N., Porcar-Castell, A., Flexas, J., Frankenberg, C., Peylin, P.,
15 Chevallier, F., Vuichard, N., and Bastrikov, V.: Improving estimates of Gross Primary
16 Productivity by assimilating solar-induced fluorescence satellite retrievals in a terrestrial
17 biosphere model using a process-based SIF model, *Journal of Geophysical Research:*
18 *Biogeosciences*, 124(11), 3281-3306, 2019.
- 19 Baker, I.T., Prihodko, L., Denning, A.S., Goulden, M., Miller, S., and da Rocha, H.: Seasonal
20 Drought Stress in the Amazon: Reconciling Models and Observations, *J.Geophys. Res.*, 113,
21 G00B01, doi:10.1029/2007JG000644, 2008.
- 22 Baker, I.T., A.S. Denning, N. Hanan, L. Prihodko, P.-L. Vidale, K. Davis and P. Bakwin: Simulated
23 and observed fluxes of sensible and latent heat and CO2 at the WLEF-TV Tower using
24 SiB2.5, *Glob. Change Biol.*, 9, 1262-1277, 2003.
- 25 Ball, J. T., Woodrow, I. E., and Berry, J. A.: A model predicting stomatal conductance and its
26 contribution to the control of photosynthesis under different environmental
27 conditions, *Progress in photosynthesis research*, Springer, Dordrecht, 221-224, 1987.
- 28 Burns, S. P., Blanken, P. D., Turnipseed, A. A., Hu, J., and Monson, R. K.: The influence of warm-
29 season precipitation on the diel cycle of the surface energy balance and carbon dioxide at
30 a Colorado subalpine forest site, *Biogeosciences*, 12, 7349–7377, 2015.
- 31 [Burns, S. P., Swenson, S. C., Wieder, W. R., Lawrence, D. M., Bonan, G. B., Knowles, J. F., and](#)
32 [Blanken, P. D.: A comparison of the diel cycle of modeled and measured latent heat flux](#)
33 [during the warm season in a Colorado subalpine forest, *Journal of Advances in Modeling*](#)
34 [Earth Systems](#), 10, 617–651, 2018.

- 1 Chen, J. M., Liu, J., Cihlar, J., and Goulden, M. L.: Daily canopy photosynthesis model through
2 temporal and spatial scaling for remote sensing applications, *Ecological Modelling*, 124(2–
3 3), 99–119, 1999.
- 4 Demmig-Adams, B., Cohu, C. M., Muller, O., and Adams, W. W.: Modulation of photosynthetic
5 energy conversion efficiency in nature: from seconds to seasons, *Photosynthesis Research*,
6 113(1–3), 75–88. <https://doi.org/10.1007/s11120-012-9761-6>, 2012.
- 7 [Dechant, B., Ryu, Y., Badgley, G., Zeng, Y., Berry, J.A., Zhang, Y., Goulas, Y., Li, Z., Zhang, Q.,
8 Kang, M., Li, J., Moya, I.: Canopy structure explains the relationship between
9 photosynthesis and sun-induced chlorophyll fluorescence in crops, *Remote Sensing of
10 Environment*, 241, 111733, 2020.](#)
- 11 Dufresne, J.-L., Foujols, M.-A., Denvil, S., Caubel, A., Marti, O., Aumont, O., Balkanski, Y., Bekki,
12 S., Bellenger, H., Benschila, R., and Bony, S.: Climate change projections using the IPSL-CM5
13 Earth System Model: from CMIP3 to CMIP5, *Climate Dynamics*, 40(9–10), 2123–2165,
14 2013.
- 15 [Eller, Cleiton B., Rowland, L., Mencuccini, M., Rosas, T., Williams, K., Harper, A., Medlyn, B. E.,
16 Wagner, Y., Klein, T., Teodoro, G.S. and Oliveira, R.S.: Stomatal optimisation based on
17 xylem hydraulics \(SOX\) improves land surface model simulation of vegetation responses to
18 climate, *New Phytologist*, 2020.](#)
- 19 Flexas, J., Escalona, J. M., Evain, S., Gulías, J., Moya, I., Osmond, C. B., and Medrano, H.: Steady-
20 state chlorophyll fluorescence (Fs) measurements as a tool to follow variations of net CO2
21 assimilation and stomatal conductance during water-stress in C3 plants. *Physiologia
22 Plantarum*, 114(2), 231–240. <https://doi.org/10.1034/j.1399-3054.2002.1140209.x>, 2002.
- 23 Friedlingstein, P., Meinshausen, M., Arora, V. K., Jones, C. D., Anav, A., Liddicoat, S. K., and
24 Knutti, R.: Uncertainties in CMIP5 climate projections due to carbon cycle feedbacks,
25 *Journal of Climate*, 27(2), 511–526, 2014.
- 26 Galmés, J., Flexas, J., Savé, R., and Medrano, H.: Water relations and stomatal characteristics of
27 Mediterranean plants with different growth forms and leaf habits: responses to water
28 stress and recovery, *Plant and Soil*, 290(1–2), 139–155, 2007.
- 29 Gastellu-Etchegorry, J. P., Malenovský, Z., Duran Gomez, N., Meynier, J., Lauret, N., Yin, T., Qi,
30 J., Guilleux, J., Chavanon, E., Cook, B., Morton, D.: Simulation of chlorophyll fluorescence
31 for sun- and shade-adapted leaves of 3D canopies with the DART model, *International
32 Geoscience and Remote Sensing Symposium (IGARSS)*, 2018-July, 5995–5998.
33 <https://doi.org/10.1109/IGARSS.2018.8517576>, 2018.
- 34 Grossmann, K., Frankenberg, C., Magney, T. S., Hurllock, S. C., Seibt, U., and Stutz, J.: PhotoSpec:
35 A new instrument to measure spatially distributed red and far-red Solar-Induced
36 Chlorophyll Fluorescence, *Remote Sensing of Environment*, 216, 311–327.
37 <https://doi.org/10.1016/j.rse.2018.07.002>, 2018.

- 1 Gu, L., Han, J., Wood, J. D., Chang, C. Y., and Sun, Y.: Sun-induced Chl fluorescence and its
2 importance for biophysical modeling of photosynthesis based on light reactions, *New*
3 *Phytologist*, nph.15796. <https://doi.org/10.1111/nph.15796>, 2019.
- 4 Gu, L., Wood, J. D., Chang, C. Y. Y., Sun, Y., and Riggs, J. S.: Advancing Terrestrial Ecosystem
5 Science With a Novel Automated Measurement System for Sun-Induced Chlorophyll
6 Fluorescence for Integration With Eddy Covariance Flux Networks, *Journal of Geophysical*
7 *Research: Biogeosciences*, 124(1), 127–146. <https://doi.org/10.1029/2018JG004742>, 2019.
- 8 Haynes, K., Baker, I. T., Denning, S., Stöckli, R., Schaefer, K., Lokupitiya, E. Y., and Haynes, J. M.:
9 Representing grasslands using dynamic prognostic phenology based on biological growth
10 stages: 1. Implementation in the Simple Biosphere Model (SiB4), *Journal of Advances in*
11 *Modeling Earth Systems*, 11. <https://doi.org/10.1029/2018MS001540>, 2019a.
- 12 Haynes, K. D., Baker, I. T., Denning, A. S., Wolf, S., Wohlfahrt, G., Kiely, G., Minaya, R. C., and
13 Haynes, J. M.: Representing grasslands using dynamic prognostic phenology based on
14 biological growth stages: 2. Carbon cycling, *Journal of Advances in Modeling Earth*
15 *Systems*, 11. <https://doi.org/10.1029/2018MS001541>, 2019b.
- 16 [Julitta, T., Burkart, A., Colombo, R., Rossini, M., Schickling, A., Migliavacca, M., Cogliati, S.,
17 Wutzler, T., Rascher, U.: Accurate measurements of fluorescence in the O2A and O2B band
18 using the FloX spectroscopy system - results and prospects. In: Proc. Potsdam GHG Flux
19 Workshop: From Photosystems to Ecosystems, 24–26 October 2017, Potsdam, Germany.
20 <https://www.potsdam-flux-workshop.eu/>, 2017](https://www.potsdam-flux-workshop.eu/)
- 21 Kaminski, T., Knorr, W., Schürmann, G., Scholze, M., Rayner, P. J., Zaehle, S., Blessing, S., Dorigo,
22 W., Gayler, V., Giering, R., and Gobron, N.: The BETHY/JSBACH carbon cycle data
23 assimilation system: Experiences and challenges, *Journal of Geophysical Research:*
24 *Biogeosciences*, 118(4), 1414–1426, 2013.
- 25 Kennedy, D., Swenson, S., Oleson, K. W., Lawrence, D. M., Fisher, R., Lola da Costa, A. C., and
26 Gentine, P.: Implementing plant hydraulics in the community land model, version
27 5, *Journal of Advances in Modeling Earth Systems*, 11(2), 485–513, 2019.
- 28 Koffi, E. N., Rayner, P. J., Scholze, M., and Beer, C.: Atmospheric constraints on gross primary
29 productivity and net ecosystem productivity: Results from a carbon-cycle data assimilation
30 system, *Global Biogeochemical Cycles*, 26(1), <https://doi.org/10.1029/2010GB003900>,
31 2012.
- 32 Koffi, E. N., Rayner, P. J., Norton, A. J., Frankenberg, C., and Scholze, M.: Investigating the
33 usefulness of satellite-derived fluorescence data in inferring gross primary productivity
34 within the carbon cycle data assimilation system, *Biogeosciences*, 12(13), 4067–4084,
35 2015.

- 1 Krinner, G., Viovy, N., de Noblet-Ducoudré, N., Ogée, J., Polcher, J., Friedlingstein, P., Ciais, P.,
2 Sitch, S., and Prentice, I. C.: A dynamic global vegetation model for studies of the coupled
3 atmosphere-biosphere system, *Global Biogeochemical Cycles*, 19(1), 2005.
- 4 Lee, J.-E., Berry, J. A., van der Tol, C., Yang, X., Guanter, L., Damm, A., Baker, I., and
5 Frankenberg, C.: Simulations of chlorophyll fluorescence incorporated into the Community
6 Land Model version 4, *Global change biology*, 21 (9), 3469-3477, 2015.
- 7 Leuning R.: A critical appraisal of a combined stomatal-photosynthesis model for
8 C₃ plants, *Plant Cell Environ*, **18**: 339–357, 1995.
- 9 Li, Z., Zhang, Q., Li, J., Yang, X., Wu, Y., Zhang, Z., Wang, S., Wang, H., and Zhang, Y.: Solar-
10 induced chlorophyll fluorescence and its link to canopy photosynthesis in maize from
11 continuous ground measurements, *Remote Sensing of Environment*, 236, 111420, 2020.
- 12 Liu, J., Chen, J. M., and Cihlar, J.: Mapping evapotranspiration based on remote sensing: An
13 application to Canada's landmass, *Water Resources Research*, 39(7), 2003.
- 14 Liu, W., Atherton, J., Möttus, M., Gastellu-Etchegorry, J. P., Malenovský, Z., Raunonen, P., et
15 al.: Simulating solar-induced chlorophyll fluorescence in a boreal forest stand
16 reconstructed from terrestrial laser scanning measurements, *Remote Sensing of
17 Environment*, (July 2018), 111274, <https://doi.org/10.1016/j.rse.2019.111274>, 2019.
- 18 Medlyn, B.E., Duursma, R.A., Eamus, D., Ellsworth, D.S., Prentice, I.C., Barton, C.V.M., Crous, K.Y.,
19 De Angelis, P., Freeman, M., and Wingate, L.: Reconciling the optimal and empirical
20 approaches to modelling stomatal conductance, *Global Change Biology*, 17: 2134–2144.
21 doi:10.1111/j.1365-2486.2010.02375.x, 2011.
- 22 Magney, T. S., Frankenberg, C., Fisher, J. B., Sun, Y., North, G. B., and Davis, T. S.: Connecting
23 active to passive fluorescence with photosynthesis : a method for evaluating remote
24 sensing measurements of Chl fluorescence, *New Phytologist*, 215(4), 1594-1608,
25 <https://doi.org/10.1111/nph.14662>, 2017.
- 26 Magney, T. S., Frankenberg, C., Köhler, P., North, G., Davis, T. S., Dold, C., Dutta, D., Fisher, J. B.,
27 Grossmann, K., Harrington, A., Hatfield, J.: Disentangling Changes in the Spectral Shape of
28 Chlorophyll Fluorescence: Implications for Remote Sensing of Photosynthesis, *Journal of
29 Geophysical Research: Biogeosciences*, 124(6), 1491-1507,
30 <https://doi.org/10.1029/2019JG005029>, 2019a.
- 31 Magney, T. S., Bowling, D. R., Logan, B., Grossmann, K., Stutz, J., and Blanken, P.: Mechanistic
32 evidence for tracking the seasonality of photosynthesis with solar-induced fluorescence,
33 *Proceedings of the National Academy of Sciences*, 116 (24), 11640-11645,
34 <https://doi.org/10.1073/pnas.1900278116>, 2019b.

1 Miguez, F., Fernández-Marin, B., Becerril, J. M., and Garcia-Plazaola, J. I.: Activation of
 2 photoprotective winter photoinhibition in plants from different environments: a literature
 3 compilation and meta-analysis, *Physiologia Plantarum*, 155(4), 414–423, 2015.

4 Mohammed, G. H., Colombo, R., Middleton, E. M., Rascher, U., van der Tol, C., Nedbal, L.,
 5 Goulan, Y., Perez-Priego, O., Damm, A., Meroni, M. and Joiner, J.: Remote sensing of solar-
 6 induced chlorophyll fluorescence (SIF) in vegetation: 50 years of progress, *Remote Sensing
 7 of Environment*, 231, 111177, <https://doi.org/10.1016/j.rse.2019.04.03>, 2019.

8 Monteith, J. L.: Solar Radiation and Productivity in Tropical Ecosystems, *J. Appl. Ecol.*, 9, 747–
 9 766, <https://doi.org/10.2307/2401901>, 1972.

10 Norton, A. J., Rayner, P. J., Koffi, E. N., and Scholze, M.: Assimilating solar-induced chlorophyll
 11 fluorescence into the terrestrial biosphere model BETHY-SCOPE v1. 0: model description
 12 and information content, *Geoscientific Model Development*, 11(4), 1517–1536, 2018.

13 Norton, A. J., Rayner, P. J., Koffi, E. N., Scholze, M., Silver, J. D., and Wan, Y.-P.: Estimating global
 14 gross primary productivity using chlorophyll fluorescence and a data assimilation system
 15 with the BETHY-SCOPE model, *Biogeosciences*, 16(15), 3069-3093, 2019.

16 Porcar-Castell, A.: A high-resolution portrait of the annual dynamics of photochemical and non-
 17 photochemical quenching in needles of *Pinus sylvestris*, *Physiologia Plantarum*, 143(2),
 18 139–153, <https://doi.org/10.1111/j.1399-3054.2011.01488.x>, 2011.

19 Qiu, B., Chen, J. M., Ju, W., Zhang, Q., and Zhang, Y.: Simulating emission and scattering of
 20 solar-induced chlorophyll fluorescence at far-red band in global vegetation with different
 21 canopy structures, *Remote Sensing of Environment*, 111373, 2019.

22 [Raczka, B., Duarte, H. F., Koven, C. D., Ricciuto, D., Thornton, P. E., Lin, J. C., & Bowling, D. R.: An
 23 observational constraint on stomatal function in forests: evaluating coupled carbon and
 24 water vapor exchange with carbon isotopes in the Community Land Model \(CLM4.
 25 5\), *Biogeosciences*, 13\(18\), 5183-5204, 2016.](#)

26 Raczka, B., Porcar-Castell, A., Magney, T., Lee, J. E., Köhler, P., Frankenberg, C., Grossman, K.,
 27 Logan, B.A., Stutz, J., Blanken, P. D., Burns, S. P., Duarte, H., Yang, X., Lin, J. C., and Bowling,
 28 D. R.: Sustained nonphotochemical quenching shapes the seasonal pattern of solar-
 29 induced fluorescence at a high-elevation evergreen forest, *Journal of Geophysical
 30 Research: Biogeosciences*, 124, 2005–2020, <https://doi.org/10.1029/2018JG004883>, 2019.

31 Rayner, P. J., Scholze, M., Knorr, W., Kaminski, T., Giering, R., and Widmann, H.: Two decades of
 32 terrestrial carbon fluxes from a carbon cycle data assimilation system (CCDAS), *Global
 33 Biogeochemical Cycles*, 19(2), 2005.

34 Schreiber, U., Schliwa, U., and Bilger, W.: Continuous recording of photochemical and non-
 35 photochemical chlorophyll fluorescence quenching with a new type of modulation
 36 fluorometer, *Photosynthesis Research*, 10, 51–62, 1986.

Formatted: Font: (Default) Calibri, 12 pt

Formatted: Font: (Default) Calibri, 12 pt

Formatted: Font: (Default) Calibri, 12 pt

Formatted: Font: (Default) Calibri, 12 pt, Not Italic

Formatted: Font: (Default) Calibri, 12 pt

1 Sellers, P. J., Randall, D. A., Collatz, G. J., Berry, J. A., Field, C. B., Dazlich, D. A., Zhang, C., Collelo,
 2 G. D., and Bounoua, L.: A revised land surface parameterization (SiB2) for atmospheric
 3 GCMs. Part I: Model formulation, *Journal of Climate*, 9(4), 676–70, 1996.

4 [Shan, N., Ju, W., Migliavacca, M., Martini, D., Guanter, L., Chen, J., Goulas, Y., Zhang, Y.:](#)
 5 [Modeling canopy conductance and transpiration from solar-induced chlorophyll](#)
 6 [fluorescence. *Agricultural and Forest Meteorology*, 268, 189–201, 2019.](#)

7 [Svishnikov, D., Ensminger, I., Ivanov, A. G., Campbell, D., Lloyd, J., Funk, C., Huner, N. P. A.,](#)
 8 [Oquist, G.: Excitation energy partitioning and quenching during cold acclimation in Scots](#)
 9 [pine. *Tree Physiology*, 26\(3\), 325-336, 2006.](#)

10 Van Der Tol, C., Berry, J. A., Campbell, P. K. E., and Rascher, U.: Models of fluorescence and
 11 photosynthesis for interpreting measurements of solar-induced chlorophyll fluorescence,
 12 *Journal of Geophysical Research: Biogeosciences*, 119(12), 2312–2327.
 13 <https://doi.org/10.1002/2014JG002713>, 2014.

14 [Wohlfahrt, G., Gerdel, K., Migliavacca, M., Rotenberg, E., Tatarinov, F., Müller, J., Hammerle,](#)
 15 [A., Julitta, T., Spielmann, F.M., Yakir, D.: Sun-induced fluorescence and gross primary](#)
 16 [productivity during a heat wave. *Sci. Rep.*, 8, 1–9, 2018.](#)

17 Yang, P., and van der Tol, C.: Linking canopy scattering of far-red sun-induced chlorophyll
 18 fluorescence with reflectance, *Remote Sensing of Environment*, 209(May), 456–467.
 19 <https://doi.org/10.1016/j.rse.2018.02.029>, 2018.

20 Yin, X., and Struik, P. C.: C3 and C4 photosynthesis models: an overview from the perspective of
 21 crop modelling, *NJAS-Wageningen Journal of Life Sciences*, 57(1), 27-38, 2009.

22 Zhang, Y., Guanter, L., Berry, J. A., van der Tol, C., Yang, X., Tang, J., and Zhang, F.: Model-based
 23 analysis of the relationship between sun-induced chlorophyll fluorescence and gross
 24 primary production for remote sensing applications, *Remote Sensing of Environment*, 187,
 25 145–155, 2016.

26 Zhang, Q., Zhang, X., Li, Z., Wu, Y., and Zhang, Y: Comparison of Bi-Hemispherical and
 27 Hemispherical-Conical Configurations for In Situ Measurements of Solar-Induced
 28 Chlorophyll Fluorescence, *Remote Sensing*, 11, 2642, 2019.

29

Formatted: Font: (Default) Calibri, 12 pt

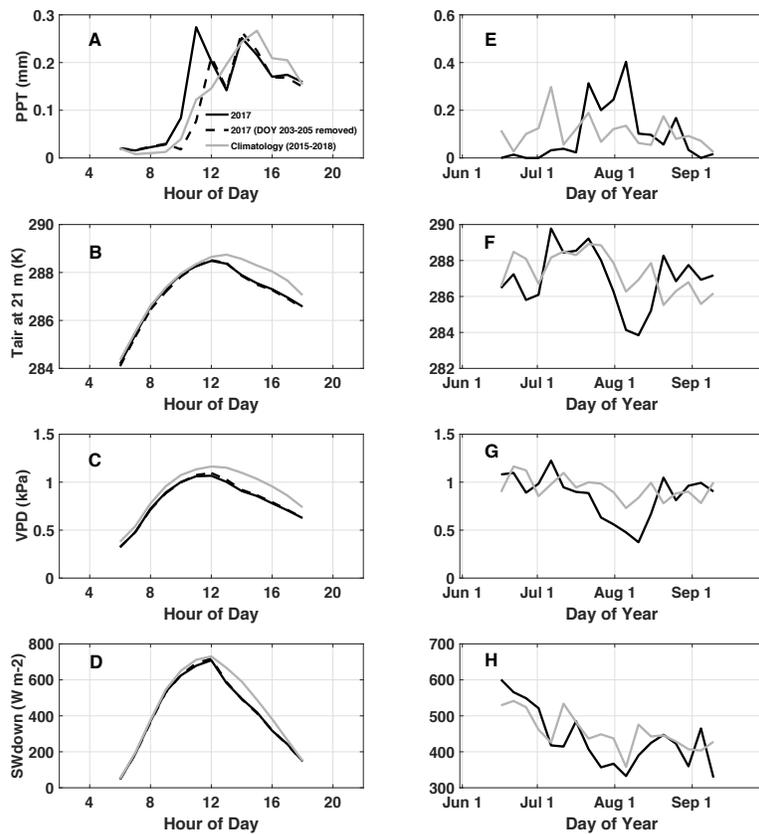
Formatted: Font: (Default) Calibri, 12 pt

Formatted: Font: (Default) Calibri, 12 pt

Deleted: ¶

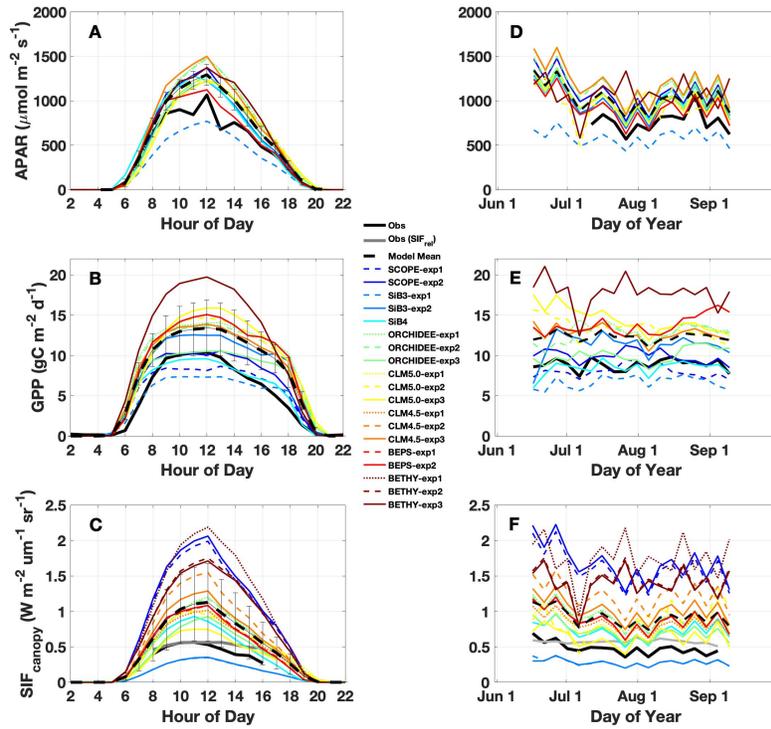
Formatted: Normal (Web), Indent: Left: 0", Hanging: 0.33"

1 Figures

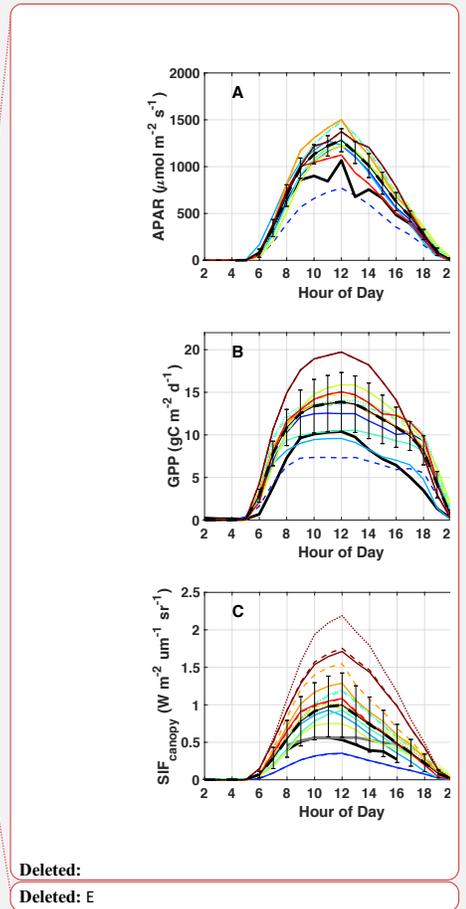


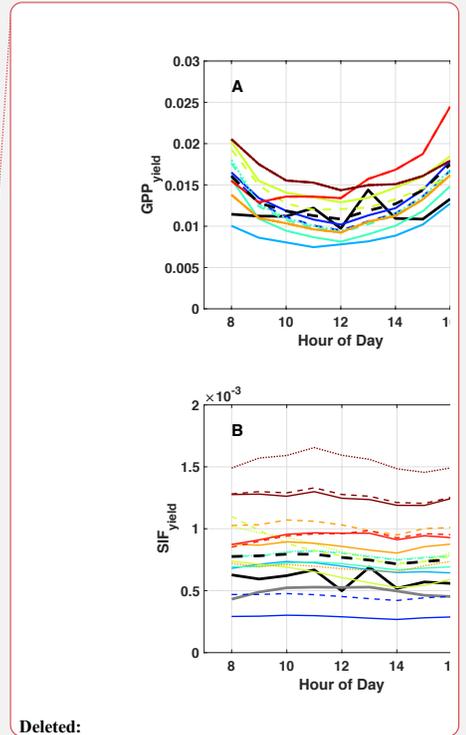
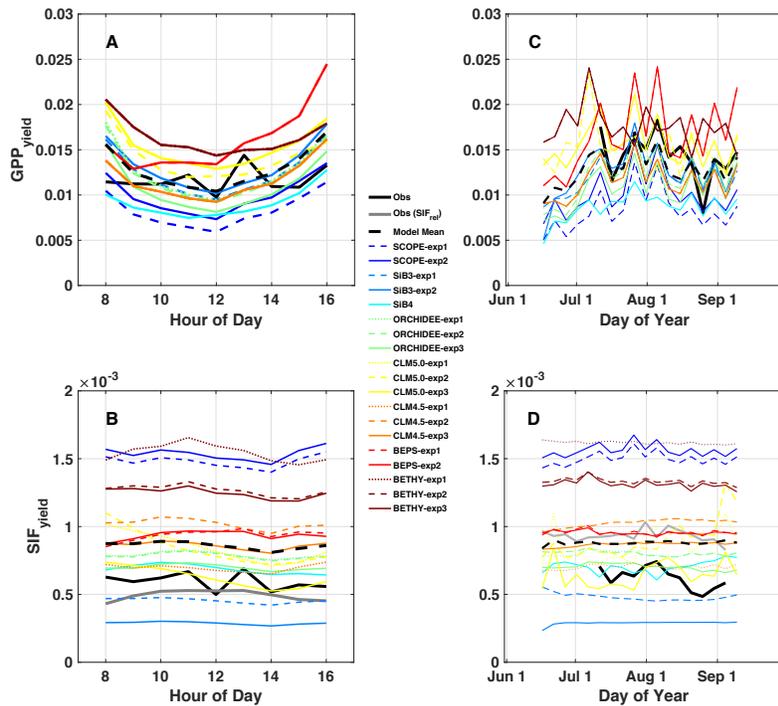
2

3 **Figure 1.** Observed diurnal (A-D) and synoptic (E-H) precipitation (PPT), air temperature at 21 m
4 (Tair), vapor pressure deficit (VPD), and downwelling shortwave (SWdown). Diurnal cycles are
5 averaged over July-August, 2017. Synoptic cycles are plotted as 5-day averages from June 15 –
6 Sep 15. Data from 2017 is shown in black and climatology (2015-2018) in grey. Typically, peak
7 rainfall occurs in the afternoon at this site (A). A substantial rain event which occurred from DOY
8 203-205 is removed from the 2017 average to show the impact on diurnal variability and to
9 demonstrate the dominance of the afternoon monsoon upon diurnal precipitation in summer.



1
 2 **Figure 2.** Observed and simulated diurnal and synoptic cycles of APAR, GPP and SIF. Diurnal cycles
 3 (A-C) are averaged over July-August, 2017. Synoptic cycles (D-F) are plotted as 5-day averages
 4 from June 15 – Sep 15. Observations are shown in black, with relative SIF (SIF_{canopy} / far red
 5 reflected radiance) included in (C, F) in grey. The across model average (dashed black) represents
 6 the average of “best-case” model scenarios (solid lines; SCOPE-exp2, SiB3-exp2, SiB4, ORCHIDEE-
 7 exp3, CLM5.0-exp3, CLM4.5-exp3, BEPS-exp2, BETHY-exp3) with uncertainty bars indicating the
 8 across model 1 sigma uncertainty.





Deleted:

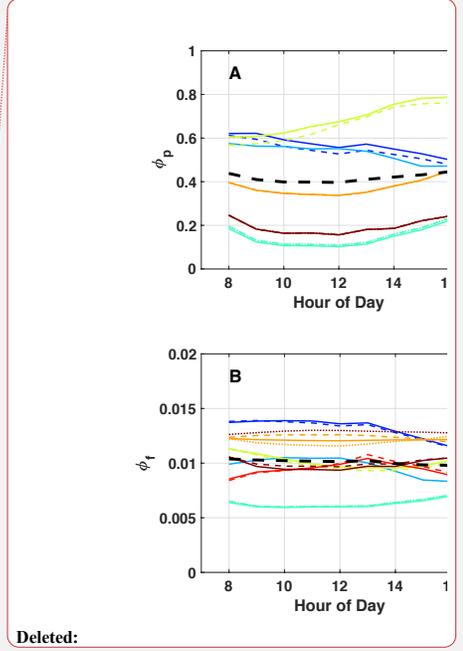
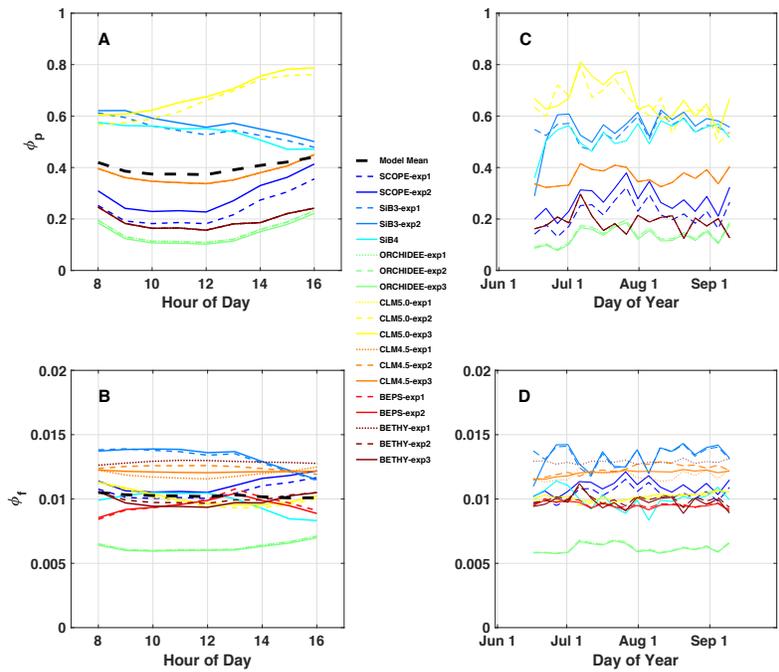
1

2 **Figure 3.** Same as Figure 2 except for SIF_{yield} and GPP_{yield}. Here, SIF_{yield} = SIF_{canopy} / APAR, and

3 GPP_{yield} = GPP / APAR. As with Figure 2, the left column shows the mean diurnal cycle, and the

4 right column shows a time series of 5-day averages.

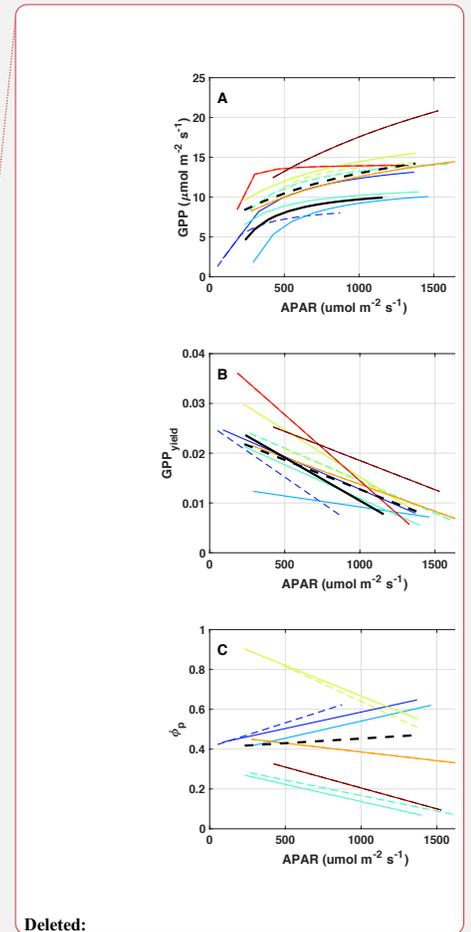
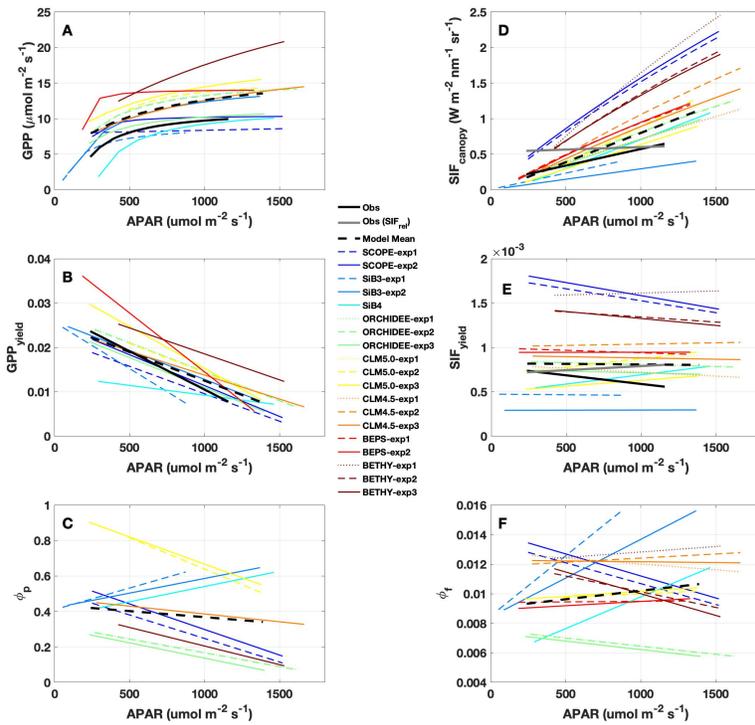
5



Deleted:

1
 2 **Figure 4.** Same as Figure 2, except for quantum yield of fluorescence (ϕ_F) and photochemistry
 3 (ϕ_P).

4
 5
 6



1
 2 **Figure 5.** Observed and predicted change in GPP, SIF, and yields with APAR. Regression lines are
 3 shown for (A) GPP, (B) $\text{GPP}_{\text{yield}}$, (C) photochemical quantum yield (ϕ_p), (D) $\text{SIF}_{\text{canopy}}$, (E) $\text{SIF}_{\text{yield}}$, (F)
 4 fluorescence quantum yield (ϕ_f), as a function of APAR, using daily mean (8 am – 4 pm local)
 5 values over the period July-August 2017. Observations are shown in solid black, individual models
 6 and experiments in color, the across model average in dashed black. Relative SIF is shown in grey
 7 in (D) and (E).

8
 9

1 **Tables**

Model (citation)	Model Experiments	Stomatal Conductance	Canopy Type / Radiation	Stress	Vcmax	LAI	k _N	Leaf-to-Canopy Scaling	Parameter Optimization	
SCOPE v1.73 (van der Tol, 2014)	SCOPE-exp1	Ball-Berry Woodrow	Multi-layer Sunlit/Shaded = Yes Fpar/APAR = semi-analytical canopy radiative model (based on SAIL)	Ta stress	Prescribed (30)	Prescribed (4.0 m ² m ⁻²)	Adapted to drought stressed Mediterranean species including high temperature correction (Tol et al., 2014; Flexas et al., 2002)	60 layer 1D radiative transfer	Hand-tuned to NR1 (Racza et al., 2016)	
	SCOPE-exp2			Seasonally calibrated to NR1						
	SCOPE-exp3									
BETHY (Norton et al., 2019)	BETHY-exp1	Ball-Berry Woodrow	Same as SCOPE	Ta stress	Prior is a function of Ta	Prescribed (4.0 m ² m ⁻²)	Adapted to unstressed cotton species (Tol et al., 2014) Adapted to drought stressed Mediterranean species including high temperature correction (Tol et al., 2014; Flexas et al., 2002) Adapted to drought stressed Mediterranean species (Flexas et al., 2002)	SCOPE radiative transfer, fTA, APAR, structure, leaf composition) via dependence of photosynthetic rate on ψ_s	Default	
	BETHY-exp2									
	BETHY-exp3									
ORCHDEE (Bacour et al., 2019)	ORCHDEE-exp1	Yin-Struik	Big Leaf Sunlit/Shaded = No APAR = Beer-Lambert law depending on LAI and extinction factor = 0.5	Ta stress	f (leaf age, CO ₂ , Ta, water stress)	Prognostic	Adapted to needleleaf species (Porcar-Castell et al., 2011) and unstressed Mediterranean species (Flexas, 2002), with added dependence on PAR, temperature, and ψ_s	Parametric representation of SCOPE (v1.61) to emulate radiative transfer within canopy for PS/II.	Default	
	ORCHDEE-exp2			Ta and water stress (Yin and Struik, 2009)	Default					
	ORCHDEE-exp3			Same as exp 1	Global ENF PFT optimized against OCO-2					
BEPS (Qiu et al., 2019)	BEPS-exp1	Leuning	Two Leaf Sunlit/Shaded = Yes Fpar = semi-analytical canopy radiative transfer	Soil water stress factor (ratio of measured soil available water to maximum plant available water)	Prescribed	Prescribed (4.0 m ² m ⁻²)	Adapted to water stressed Mediterranean species (Galmes et al., 2007) Adapted to drought stressed Mediterranean species including high temperature correction (Tol et al., 2014; Flexas et al., 2002)	Parametric representation of radiative transfer physics to account for canopy scattering effects	Default	
	BEPS-exp2									
CLM4.5 (Racza et al., 2019)	CLM4.5-exp1	Ball-Berry Woodrow	Two Big Leaf Sunlit/Shaded = Yes	Ta(Vcmax); soil moisture stress uses Bran parameterization (function of column rooting profile and soil water potential)	Prescribed (calibrated against observed GPP at NR1)	Prescribed (4.0 m ² m ⁻²)	Adapted to water stressed Mediterranean species (Galmes et al., 2007) Adapted to needleleaf species (Porcar-Castell et al., 2011); Accounts for sustained NPQ (k _N) separately from reversible NPQ (k _r). k _r is calibrated to NR1. Ta _r is fixed in time same as Exp 2, but k _r is seasonal	k _N = f(Vcmax, SZA), calibrated to offline SCOPE runs using prescribed canopy characteristics at NR1	Hand-tuned to NR1 (Racza et al., 2016)	
	CLM4.5-exp2									
	CLM4.5-exp3									
CLM5.0 (unpublished)	CLM5.0-exp1	Medlyn	Two Big Leaf Sunlit/Shaded = Yes	Plant hydraulic water stress (Sperry and Love, 2015; Lawrence et al., 2019) accounting for water demand and supply	f (soil moisture, nitrogen, calibrated to NR1)	Prescribed (4.0 m ² m ⁻²)	Adapted to water stressed Mediterranean species (Galmes et al., 2007)	k _N = f(Vcmax), calibrated to offline SCOPE runs from Lee et al. (2015) k _N = f(Vcmax, SZA), calibrated to offline SCOPE runs w/ prescribed canopy characteristics at NR1 Escape ratio (f _{esc}) derived from NIRv and IPAR (Zeng et al., 2019)	Default	
	CLM5.0-exp2									
	CLM5.0-exp3									
SIB3 (Baker et al., 2003, 2008) SIB4 (Haynes et al., 2019a,b)	SIB3-exp1	Ball-Berry Woodrow	Big Leaf Sunlit/Shaded = No	Downregulation by VPD, Ta, and soil moisture	f (soil moisture)	Prescribed (MCD05)	Adapted to drought stressed species (Tol et al., 2014)	k _N = f(Vcmax), calibrated to offline SCOPE runs from Lee et al. (2015)	Default	
	SIB3-exp2				Prescribed (4.0 m ² m ⁻²)					
	SIB4				Prognostic					

2

3 **Table 1.** Summary of TBM-SIF models and within model experiments illustrating model
 4 components that may have led to differences in modeled SIF., These include a representation of
 5 stomatal-conductance (column 3), canopy absorption of incoming radiation (column 4), limiting
 6 factors for photosynthesis (Stress, V_{cmax}, LAI; columns 5-7) and SIF (k_N; column 8), leaf-to-canopy
 7 scaling of SIF (column 9), and parameter optimization (column 10). The underlined model
 8 experiment was used for model intercomparison.

9

10

11

Model (TBM-SIF reference)	Model Experiments	Stomatal Conductance	Canopy Type / Radiation	Stress
BETHY (Norton et al., 2019)	BETHY-exp1	Ball-Berry	Multiple Layers Sunlit/Shaded = Yes Fpar/APAR = semi-analytical canopy radiative model (SCOPE, based on SAIL)	Ta and water stress
	BETHY-exp2			
	BETHY-exp3			
ORCHDEE (Bacour et al., 2019)	ORCHDEE-exp1	Yin-Struik	Big Leaf Model Sunlit/Shaded = No APAR = Beer-Lambert law depending on LAI and extinction factor = 0.5	Ta stress
	ORCHDEE-exp2			
	ORCHDEE-exp3			
BEPS (Qiu et al., 2019)	BEPS-exp1	Ball-Berry-Leuning	Single Layer Sunlit/Shaded = Yes Fpar = semi-analytical canopy radiative transfer	Soil water stress factor (ratio of measured soil available water to maximum plant available water)
	BEPS-exp2			
CLM4.5 (Racza et al., 2019)	CLM4.5-exp1	Ball-Berry	Single Layer Sunlit/Shaded = Yes	Ta(Vcmax); soil moisture stress uses Bran parameterization (function of column rooting profile and soil water potential)
	CLM4.5-exp2			
	CLM4.5-exp3			
CLM5.0 (unpublished)	CLM5.0-exp1	Medlyn	Single Layer Sunlit/Shaded = Yes	Plant hydraulic water stress (Sperry and Love, 2015; Lawrence et al., 2019) accounting for water demand and supply
	CLM5.0-exp2			
	CLM5.0-exp3			
SIB3 (Baker et al., 2003, 2008) SIB4 (Haynes et al., 2019a,b)	SIB3-exp1	Ball-Berry	Single Layer Sunlit/Shaded = Yes	Downregulation by VPD, Ta, and soil moisture
	SIB3-exp2			
	SIB4			

Deleted: